



# CHORUS

This is the accepted manuscript made available via CHORUS. The article has been published as:

## Search-and-capture model of cytoneme-mediated morphogen gradient formation

Paul C. Bressloff and Hyunjoong Kim

Phys. Rev. E **99**, 052401 — Published 1 May 2019

DOI: [10.1103/PhysRevE.99.052401](https://doi.org/10.1103/PhysRevE.99.052401)

# Search-and-capture model of cytoneme-mediated morphogen gradient formation

Paul C. Bressloff and Hyunjoong Kim

*Department of Mathematics, University of Utah 155 South 1400 East, Salt Lake City, UT 84112*

Morphogen protein gradients play an essential role in the spatial regulation of patterning during embryonic development. The most commonly accepted mechanism of protein gradient formation involves the diffusion and degradation of morphogens from a localized source. Recently, an alternative mechanism has been proposed, which is based on cell-to-cell transport via thin, actin-rich cellular extensions known as cytonemes. Very little is currently known about the precise nature of the contacts between cytonemes and their target cells. Important unresolved issues include how cytoneme tips find their targets, how they are stabilized at their contact sites, and how vesicles are transferred to a receiving cell and subsequently internalized. It has been hypothesized that cytonemes find their targets via a random search process based on alternating periods of retraction and growth, perhaps mediated by some chemoattractant. This is an actin-based analog of the search-and-capture model of microtubules of the mitotic spindle searching for cytochrome binding sites (kinetochores) prior to separation of cytochrome pairs. In this paper, we develop a search-and-capture model of cytoneme-based morphogenesis, in which nucleating cytonemes from a source cell dynamically grow and shrink along the surface of a one-dimensional array of target cells until making contact with one of the target cells. We analyze the first passage time problem for making contact, and then use this to explore the formation of morphogen gradients under the mechanism proposed for Wnt in vertebrates. That is, we assume that morphogen is localized at the tip of a growing cytoneme, which is delivered as a “morphogen burst” to a target cell when the cytoneme makes temporary contact with a target cell before subsequently retracting. We show how multiple rounds of search-and-capture, morphogen delivery, cytoneme retraction and nucleation events lead to the formation of a morphogen gradient. We proceed by formulating the morphogen bursting model as a queuing process, analogous to the study of translational bursting in gene networks. In order to analyze the expected times for cytoneme contact, we introduce a new efficient method for solving first passage time problems in the presence of sticky boundaries, which exploits some classical concepts from probability theory, namely, stopping times and the strong Markov property. We end the paper by demonstrating how this method simplifies previous analyses of a well-studied problem in cell biology, namely, the search-and-capture model of microtubule/kinetochore attachment. Although the latter is completely unrelated to cytoneme-based morphogenesis from a biological perspective, it shares many of the same mathematical elements.

## I. INTRODUCTION

Cytonemes are thin, dynamic, actin-rich cellular extensions with a diameter of around 100 nm and lengths that vary from 1 to 100  $\mu\text{m}$ . There is growing experimental evidence that cytonemes can form direct cell-to-cell contacts, thus allowing the active transport of morphogens or their cognate receptors to embryonic cells during development [1–10]. Recent modeling studies have investigated how the number of morphogens or receptors delivered to a cell depends on the flux of particles along a cytoneme, the number of cytonemes that form a stable contact with the target cell, and the duration of each contact [11–13]. However, very little is still known about the precise biochemical and physical nature of the contacts between cytonemes and their target cells. Important unresolved issues include how cytoneme tips find their targets, how they are stabilized at their contact sites, and how vesicles are transferred to a receiving cell and subsequently internalized. It has been hypothesized that cytonemes find their targets via a random search process based on alternating periods of retraction and growth, perhaps mediated by some chemoattractant [5]. Indeed, imaging studies in *Drosophila* [3] and chick [4] show that cytonemes actively and rapidly expand and

contract. This is analogous to the search-and-capture model of microtubules of the mitotic spindle searching for cytochrome binding sites (kinetochores) prior to separation of cytochrome pairs [14–16], although one major difference is that cytonemes are actin-based rather than tubulin-based.

Once a cytoneme contact has been established, a number of different mechanisms have been proposed for how vesicles containing morphogens (or their cognate receptors) are delivered to the target cell. In the wing imaginal disc of *Drosophila* vesicles appear to be actively transported along the cytonemes in a bidirectional fashion, probably via myosin motors that actively “walk” along the actin filaments of a cytoneme [1–3]. The amount of morphogen delivered to a cell will then depend on the flux of particles along a cytoneme and the number of cytonemes that form a stable contact with the target cell. Increasing experimental evidence indicates that cytonemes also mediate morphogen transport in vertebrates [7, 10]. Examples include sonic hedgehog (Shh) cell-to-cell signaling in chicken limb buds [4] and Wnt signaling in zebrafish [8, 9]. The latter is thought to involve a different morphogen transport mechanism, in which Wnt is clustered at the membrane tip of growing signaling filopodia. When the filopodia make contact

with target cells, the morphogens are delivered to the cells and the filopodia are pruned off within 10 minutes of making contact. In this case, the amount of morphogen delivered to a cell will depend on the rate of filopodia growth, the concentration of morphogen at the tips, and the frequency of contacts between source and target cells.

Dynamic instabilities in microtubules are much better understood than in cytonemes. Microtubules grow by the attachment of guanosine triphosphate (GTP)-tubulin complexes at one end. In order to maintain growth, the end of the microtubule must consist of a “cap” of consecutive GTP-tubulin monomers. However, each polymerized complex can hydrolyze into guanosine diphosphate (GDP)-tubulin such that if all the monomers in the cap convert to GDP, then the microtubule is destabilized, and there is rapid shrinkage due to detachment of the GDP-tubulin monomers. The competition between attachment of GTP-tubulin and hydrolysis from GTP to GDP is thought to be the basic mechanism of alternating periods of growth and shrinkage [17, 18]. The search-and-capture model of cell mitosis involves the nucleation of microtubules in random directions, which then grow and shrink dynamically in order to search space and eventually encounter a target kinetochore [14–16]. A number of recent modeling studies have analyzed search-and-capture in terms of a first passage time problem for a velocity jump process [19–22]. One of the interesting features addressed by several of these studies is the presence of so-called *sticky boundaries* [19, 20]. For example, when a growing microtubule hits the cell membrane it can stick to the wall until it transitions to a catastrophe state after some exponentially distributed waiting time. One can also take into account the finite time for nucleation of a new growing microtubule by imposing a sticky boundary condition at the nucleation site [19]. (Very similar mathematical models arise in the case of bacterial chemotaxis, where sticky boundary conditions reflect the fact that bacteria can temporarily stick to the sides of a container [23].)

One of the difficult features of a sticky boundary condition from a mathematical perspective is that when calculating a mean first passage time (MFPT), for example, it is necessary to keep track of each time the system hits the sticky boundary before eventually exiting. As in the case of diffusion processes [24], there are two standard and complementary approaches to calculating the MFPT. The first is to determine the Green’s functions of the forward differential Chapman-Kolmogorov (CK) equation (the analog of the Fokker-Planck equation) using Laplace transforms, and to express the conditional FPT distributions in terms of these Green’s functions. In the presence of sticky boundaries, it is necessary to sum over all possible paths, after indexing them according to the number of times they visit the sticky boundary [19]. The second method is to introduce an appropriate set of splitting probabilities and conditional MFPTs and to derive differential equations for these various quantities using the backward CK equation [20]. Although the

latter direct method neatly avoids the need to sum over paths in the case of sticky boundaries, the analysis is still quite involved, particularly when extended to more complicated first passage time problems, such as those that arise in the search-and-capture model of cell mitosis.

In this paper we develop a search-and-capture model of cytoneme-mediated morphogen gradient formation, in which nucleating cytonemes from a source cell dynamically grow and shrink along the surface of a one-dimensional array of target cells until making contact with one of the target cells. We analyze the first passage time problem for making contact, and then use this to explore the formation of morphogen gradients under the mechanism proposed for Wnt in vertebrates. That is, we assume that morphogen is localized at the tip of a growing cytoneme, which is delivered as a “morphogen burst” to a target cell when the cytoneme makes temporary contact with a target cell before subsequently retracting. We then show how multiple rounds of search-and-capture, morphogen delivery, cytoneme retraction and nucleation events lead to the formation of a morphogen gradient. We proceed by formulating the morphogen bursting model as a queuing process, analogous to the study of translational bursting in gene networks [25].

Although the search-and-capture models of cytoneme-based morphogenesis and cell mitosis are completely unrelated from a biological perspective, they share several of the same mathematical elements. In particular, determining the MFPT for a single cytoneme to make contact with a target cell requires solving a first passage time problem in the presence of sticky boundaries, very similar to the MFPT for a microtubule to find a target kinetochore. In this paper we introduce a new efficient method for solving this class of first passage time problems, which exploits some classical concepts from probability theory, namely, stopping times and the strong Markov property [26]. We have previously used this approach within the context of diffusion in domains with randomly switching boundaries [27, 28]. For example, consider a Brownian particle diffusing in a two-dimensional bounded domain with a finite number of small  $O(\epsilon)$  pores distributed on the boundary of the domain. Furthermore, suppose that the pores are stochastically gated so that they randomly and independently switch between an open and a closed state. This means that one has to solve a boundary value problem in which the bulk of the boundary is reflecting, but each  $O(\epsilon)$  pore randomly switches between an absorbing and a reflecting boundary. Hence, in order to determine the MFPT to escape through an open pore, it is necessary to keep track of all prior visits to each pore when it is in a closed state. This is analogous to keeping track of visits to a sticky boundary.

The structure of the paper is as follows. In Sect. II we introduce our probabilistic method for analyzing first passage time problems with sticky boundaries by considering a filament undergoing dynamical instabilities in a bounded interval. We calculate the MFPT to hit one end of the interval, given a sticky or nucleating boundary at

the other end. We show how the MFPT can be straightforwardly expressed in terms of the splitting probabilities and conditional MFPT obtained when the sticky boundary is replaced by an absorbing boundary. In section III we introduce our search-and-capture model of a single cytoneme nucleating from a source cell and making contact at some point along a one-dimensional array of target cells. We extend the analysis of section II in order to determine the MFPT for forming such a contact. In section IV, we use queuing theory to analyze a bursting model of morphogen gradient formation. Finally, in section V we show how the probabilistic methods introduced in the paper can be used to simplify previous analyses of the search-and-capture model of microtubule/microtubule attachment. A basic introduction to stopping times and strong Markov property is presented in appendix A, and various formulae used in section III are derived in appendix B.

## II. FIRST PASSAGE TIME PROBLEM FOR A DYNAMIC FILAMENT.

Consider a filament fixed at one end ( $x = 0$ ) of a bounded domain  $[0, L]$  and let  $X(t) \in [0, L]$  be the position of the filament tip or, equivalently the filament length. Suppose that the filament can randomly switch between a growing state with tip velocity  $v_+$  and a shrinking state with tip velocity  $-v_-$ ,  $v_{\pm} > 0$ . Let  $N(t)$  denote the current velocity state, with  $N(t) = -$  if  $v(t) = -v_-$  and  $N(t) = +$  if  $v(t) = v_+$ . In other words, the position of the tip evolves according to the piecewise deterministic differential equation (velocity jump process)

$$\frac{dX(t)}{dt} = v_n, \quad N(t) = n. \quad (2.1)$$

Eq.(2.1) holds between jumps in the velocity state  $N(t)$ , which are taken to occur via a two-state Markov chain:

$$\{-\} \xrightleftharpoons[\alpha_-]{\alpha_+} \{+\}.$$

In the physics literature, this is known as a dichotomous noise process [29]. Let  $p_n(x, t)$  be the probability density that at time  $t$  we have  $x < X(t) < x + dx$  and  $N(t) = n$ . That is, for a given set of initial conditions,  $p_n(x, t) = p(x, n, t|y, m, 0)$ , where

$$p(x, n, t|y, m, 0)dx = \mathbb{P}[x \leq X(t) \leq x + dx, N(t) = n|X(0) = y, N(0) = m],$$

and  $p_n(x, 0) = \delta(x - y)\delta_{n,m}$ . The density  $p_n$  evolves according to the differential Chapman Kolmogorov (CK) equation [30, 31]

$$\frac{\partial p_+}{\partial t} = -v_+ \frac{\partial p_+}{\partial x} + \alpha_+ p_- - \alpha_- p_+ \quad (2.2a)$$

$$\frac{\partial p_-}{\partial t} = v_- \frac{\partial p_-}{\partial x} - \alpha_+ p_- + \alpha_- p_+. \quad (2.2b)$$

for  $x \in [0, L]$ . Eqs. of the form (2.2a) and (2.2b) arise in a wide range of biological applications. First, it has been used to model dynamic instabilities of microtubules known as catastrophes [18, 32], which is the closest to the application considered in this paper, namely the growth and shrinkage of cytonemes during morphogenesis. Alternatively,  $X(t)$  could represent the position of a bacterium undergoing a 1D version of run-and-tumble [23, 33, 34], or a molecular motor performing bidirectional transport along a microtubule filament [31].

In the case of confined growth and shrinkage, it is necessary to specify the boundary conditions at  $x = 0, L$ . Following previous studies of microtubular catastrophes [19, 20], we will assume that there is a reflecting boundary at  $x = L$ , so that

$$v_+ p_+(L, t) = v_- p_-(L, t), \quad (2.3)$$

and a sticky boundary at  $x = 0$ , see Fig. 1. The latter takes into account the finite time for nucleation of a new growing filament at  $x = 0$ , which occurs at some rate  $r_0$ . The sticky boundary condition is given by

$$v_+ p_+(0, t) = r_0 P_0(t), \quad (2.4)$$

where  $P_0(t)$  is the probability that the filament has shrunk to zero and is in the nucleating state at time  $t$ . The latter evolves according to the equation

$$\frac{dP_0}{dt} = v_- p_-(0, t) - r_0 P_0(t), \quad (2.5)$$

The normalization condition for the total probability is

$$\int_0^L p(x, t) dx + P_0(t) = 1. \quad (2.6)$$

A natural quantity of interest is the MFPT to hit the boundary at  $x = L$ , say, given an initial state  $X(0) = y$  and a sticky boundary at  $x = 0$ , see Eq. (2.4) and Fig. 1. One of the difficult features of a sticky boundary is that it is necessary to keep track of each time the particle hits  $x = 0$  before eventually exiting at  $x = L$ , since the particle spends an exponentially distributed time  $\tilde{\tau}_n$  in the state before reentering the growth phase. One

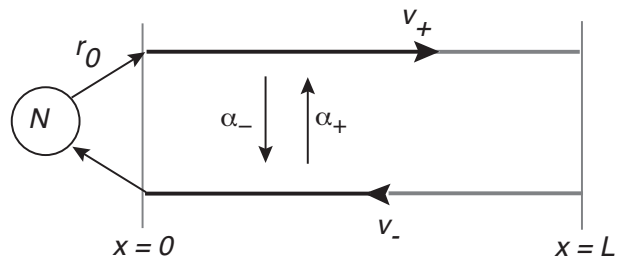


FIG. 1. Schematic representation of a sticky boundary at  $x = 0$ , with  $r_0$  the nucleation rate for switching to a growth state.

approach to calculating the MFPT is to analyze the forward CK Eqs. (2.2a) and (2.2b) using Laplace transforms and to sum over all possible paths that eventually escape at  $x = L$  [19]. However, this is a non-trivial calculation, particularly when extended to a search-and-capture model. A more direct approach, which avoids the need to perform a sum-over-paths, is to start from the backward CK equation and to derive differential equations for various splitting probabilities and conditional MFPTs [20]. In this section we show that a more efficient direct method for calculating the MFPT is to use some classical concepts from probability theory, namely, stopping times and the strong Markov property, which are summarized in appendix A. This will allow us to express the MFPT in terms of the splitting probabilities and conditional MFPT obtained when the sticky boundary at  $x = 0$  is replaced by an absorbing boundary; we consider this latter problem first, see also [20].

### A. MFPT to hit the wall at $x = L$ with an absorbing boundary at $x = 0$ .

We begin by calculating the conditional MFPT that the particle hits the wall at  $x = L$  before ever reaching zero. This means imposing absorbing boundaries at  $x = 0, L$ ,

$$p_+(0, t) = p_-(L, t) = 0,$$

and defining

$$\begin{aligned} T_m(y) &= \inf\{t \geq 0; X(t) = L \mid 0 \notin \{X(s), 0 \leq s \leq t\}\}, \\ X(0) &= y, N(0) = m \end{aligned}$$

for  $0 < y < L$ , with  $T_+(L) = 0$  (immediate absorption if the particle starts out at  $x = L$  and is in the velocity state  $v_+$ ). The probability flux through the end  $x = L$  is

$$J_m(y, t) = v_+ p_+(L, t \mid y, m, 0).$$

It follows that for  $0 < y < L$ , the probability  $\Pi_m(y, t)$  that the particle exits at  $x = L$  after time  $t$ , having started in state  $(y, m)$  is

$$\Pi_m(y, t) = \int_t^\infty J_m(y, t') dt'. \quad (2.7)$$

Differentiating with respect to  $t$  gives

$$\frac{\partial \Pi_m(y, t)}{\partial t} = -J_m(y, t) = \int_t^\infty \frac{\partial J_m(y, t')}{\partial t'} dt'.$$

Hence, using the backward CK equation leads to the pair of equations

$$\frac{\partial \Pi_+}{\partial t} = v_+ \frac{\partial \Pi_+}{\partial y} - \alpha_- [\Pi_+ - \Pi_-], \quad (2.8a)$$

$$\frac{\partial \Pi_-}{\partial t} = -v_- \frac{\partial \Pi_-}{\partial y} + \alpha_+ [\Pi_+ - \Pi_-], \quad (2.8b)$$

In order to determine the boundary conditions at  $x = 0, L$  note that if the particle starts out in the negative velocity state at  $x = 0$ , it never reaches  $x = L$ , whereas if it starts out at  $x = L$  in the positive velocity state it is immediately absorbed. Hence,  $\Pi_-(0, t) = 0$  and  $\Pi_+(L, t) = 1$ .

We can now define the hitting or splitting probability that the particle hits  $x = L$  before  $x = 0$  according to  $\pi_m(y) = \Pi_m(y, 0)$ . Since  $\partial_t \Pi_m(y, t)|_{t=0} = -J_m(y, 0) = 0$  for  $0 < y < L$ , we see that  $\pi_m$  satisfies the steady-state equations

$$0 = v_+ \frac{\partial \pi_+}{\partial y} - \alpha_- [\pi_+ - \pi_-], \quad (2.9a)$$

$$0 = -v_- \frac{\partial \pi_-}{\partial y} + \alpha_+ [\pi_+ - \pi_-], \quad (2.9b)$$

with boundary conditions  $\pi_-(0) = 0$  and  $\pi_+(L) = 1$ . It also follows that the probability that the particle hits  $x = L$  after time  $t$ , conditioned on not reaching zero, is  $\mathbb{P}[T_m(y) > t \mid T_m(y) < \infty] = \Pi_m(y, t) / \Pi_m(y, 0)$ . Since the conditional MFPT satisfies

$$\begin{aligned} \omega_m(y) &:= \mathbb{E}[T_m(y) \mid T_m(y) < \infty] \\ &= - \int_0^\infty t \frac{\partial \mathbb{P}[T_m(y) > t \mid T_m(y) < \infty]}{\partial t} dt \\ &= \int_0^\infty \frac{\Pi_m(y, t)}{\Pi_m(y, 0)} dt, \end{aligned}$$

Integrating Eqs. (2.8) with respect to  $t$  then gives

$$-\pi_+ = v_+ \frac{\partial \pi_+ \omega_+}{\partial y} - \alpha_- [\pi_+ \omega_+ - \pi_- \omega_-], \quad (2.10a)$$

$$-\pi_- = -v_- \frac{\partial \pi_- \omega_-}{\partial y} + \alpha_+ [\pi_+ \omega_+ - \pi_- \omega_-], \quad (2.10b)$$

with boundary conditions  $\pi_-(0) \omega_-(0) = \pi_+(L) \omega_+(L) = 0$ . A similar analysis can be carried out for exit through the other end  $x = 0$ . We denote the corresponding splitting probability and conditional MFPT for escape at  $x = 0$  by  $\bar{\pi}_m(y)$  and  $\bar{\omega}_m(y)$ . Note that explicit expressions for the various splitting probabilities and conditional MFPTs can be found in Ref. [20].

### B. MFPT to hit the wall at $x = L$ with a sticky boundary at $x = 0$ .

Now suppose that we include a sticky boundary at  $x = 0$  and impose the sticky boundary condition (2.4), see Fig. 1. We introduce the following set of FPTs:

$$\begin{aligned} T &= \inf\{t \geq 0; X(t) = L\}, \\ S &= \inf\{t \geq 0; X(t) = 0\}, \\ \mathcal{R} &= \inf\{t \geq 0; X(S+t) = L\}, \end{aligned}$$

where we have suppressed the dependence on the initial condition  $(y, m)$ . Introducing the set  $\Omega = \{S < T\}$ , we

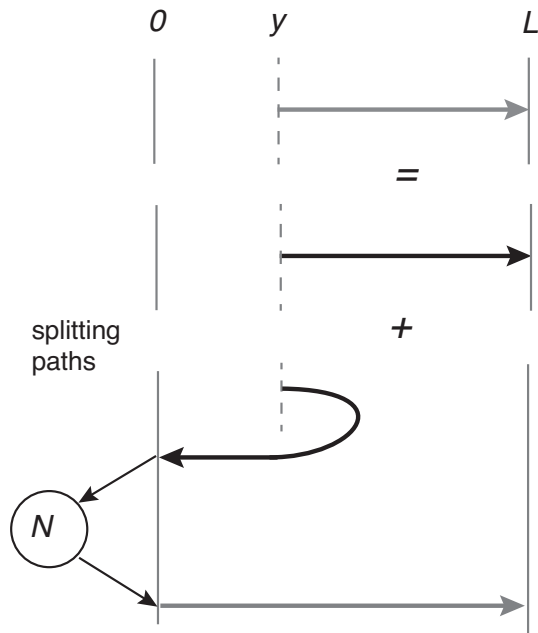


FIG. 2. Schematic diagram illustrating how the unconditional MFPT (gray arrow) for a particle to reach the boundary at  $x = L$ , starting at position  $y$ , can be split into two conditional MFPTs. The first involves all direct paths (black arrows) from  $y$  to the boundary at  $L$  (ie paths that never hit  $x = 0$ ), whereas the second involves all paths that shrink to zero length without reaching the boundary at  $x = L$ , spend some time in the state  $N$ , and then attempt to reach the boundary at  $x = L$ , starting unconditionally from zero.

can decompose the MFPT to escape at  $x = L$  according to

$$\begin{aligned} \tau &:= \mathbb{E}[T] = \mathbb{E}[T1_{\Omega^c}] + \mathbb{E}[T1_{\Omega}] \\ &= \mathbb{E}[T1_{\Omega^c}] + \mathbb{E}[(\mathcal{S} + \tilde{\tau}_n + \mathcal{R})1_{\Omega}]. \end{aligned} \quad (2.11)$$

Here  $\Omega^c$  is the complementary set of  $\Omega$  and  $1_{\Omega}$  is an indicator function which ensures that expectation is only taken with respect to events that lie in  $\Omega$ . Note that  $\mathbb{E}[T1_{\Omega^c}]$  is the MFPT that the particle hits  $x = L$  before ever hitting  $x = 0$ , and  $\mathbb{E}[\mathcal{S}1_{\Omega}]$  is the MFPT that the particle hits  $x = 0$  before ever hitting  $x = L$ . Moreover,

$$\mathbb{E}[\tilde{\tau}_n 1_{\Omega}] = \mathbb{E}[\tilde{\tau}_n] \mathbb{P}(\Omega) = r_0^{-1} \mathbb{P}(\Omega),$$

where  $r_0$  is the nucleation rate and  $\mathbb{P}(\Omega)$  is the splitting probability to hit  $x = 0$  before  $x = L$ . Incorporating the dependence on the initial conditions, we thus find  $\mathbb{P}(\Omega) = \bar{\pi}_m(y)$  and

$$\tau_m(y) = \pi_m(y)\omega_m(y) + \bar{\pi}_m(y) \left[ \bar{\omega}_m(y) + \frac{1}{r_0} \right] + \mathbb{E}[\mathcal{R}_m(y)1_{\Omega}].$$

We now exploit an important property of the velocity-jump process, namely, it satisfies the strong Markov property, which is defined in appendix A. In terms of our current example, the strong Markov property implies

that even though the stopping time  $\mathcal{S}$  is random, the stochastic process  $\hat{X}(t') = X(t - \mathcal{S})$  with times  $t' \geq 0$  is identical to the original stochastic process  $X(t)$  with the initial condition  $\hat{X}(0) = X(\mathcal{S})$ . In particular, the MFPT for  $\hat{X}$  to reach the boundary at  $x = L$  is simply  $\tau_+(0)$ , so that

$$\mathbb{E}[\mathcal{R}_m(y)1_{\Omega}] = \bar{\pi}_m(y)\tau_+(0).$$

Hence,

$$\tau_m(y) = \pi_m(y)\omega_m(y) + \bar{\pi}_m(y) \left[ \bar{\omega}_m(y) + \frac{1}{r_0} + \tau_+(0) \right]. \quad (2.12)$$

The unknown constant  $\tau_+(0)$  can be determined self-consistently by setting  $y = 0$  and  $m = +$ :

$$\tau_+(0) = \pi_+(0)\omega_+(0) + \bar{\pi}_+(0) \left[ \bar{\omega}_+(0) + \frac{1}{r_0} + \tau_+(0) \right].$$

Rearranging the equation and using  $\pi_+(0) + \bar{\pi}_+(0) = 1$  yields

$$\tau_+(0) = \omega_+(0) + \frac{\bar{\pi}_+(0)}{\pi_+(0)} \left[ \bar{\omega}_+(0) + \frac{1}{r_0} \right].$$

We thus recover Eqs. (43) and (44) of Ref. [20], which completely determine the MFPT. Following [20], the interpretation of Eq. (2.12) can be summarized diagrammatically, as illustrated in Fig. 2.

### III. SEARCH-AND-CAPTURE MODEL FOR A SINGLE CYTONEME AND MULTIPLE TARGETS

Consider a one-dimensional array of  $K + 1$  cells of size  $l$  labeled by  $k = 0, 1, \dots, K$ , see Fig. 3. A source cell  $k = 0$  projects a cytoneme that actively grows and shrinks until it forms a contact with one of the target cells. We assume that one end of the cytoneme is fixed at  $x = 0$  (a site on the source cell), and the position of the other end is

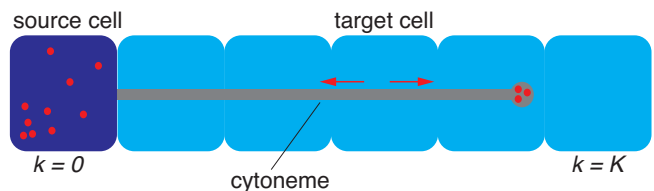


FIG. 3. One-dimensional search-and-capture model of a single cytoneme with multiple targets. For simplicity, the cytoneme is taken to dynamically grow and shrink along the surface of a one-dimensional array of cells until it eventually forms a contact with the  $k$ th cell. If the cytoneme shrinks to zero then a new cytoneme starts to grow following a nucleation waiting time.

taken to be a stochastic variable  $X(t)$ , which can also be identified as the length of the cytoneme. We take  $X(t)$  to evolve according to a slightly modified version of the two-state velocity process considered in section II. Let  $p_n(x, t)$  be the probability density that at time  $t$  the end of the cytoneme is at  $X(t) = x$  and in the discrete state  $N(t) = n$ . The corresponding CK equation is taken to be

$$\frac{\partial p_+}{\partial t} = -v_+ \frac{\partial p_+}{\partial x} - [\alpha_- + \alpha_0]p_+ + \alpha_+ p_-, \quad (3.1a)$$

$$\frac{\partial p_-}{\partial t} = v_- \frac{\partial p_-}{\partial x} + \alpha_- p_+ - [\alpha_+ + \alpha_0]p_-, \quad (3.1b)$$

for  $0 < x < L$  where  $L = Kl$ . Here  $v_+$  and  $v_-$  are the average speeds of growth and shrinkage. In contrast to the standard Dogterom-Leibler model, we also allow for the possibility that the cytoneme can be captured by a target cell anywhere in the domain  $[0, L]$  with a capture rate  $\alpha_0$ . For the moment we treat this capture event as irreversible, that is, the search-and-capture process is terminated. (When we consider a multi-cytoneme model, we will need to keep track of the subsequent retraction of the cytoneme.)

We will impose the same boundary conditions as section II, namely, the reflecting boundary condition (2.3) at  $x = L$  and the sticky boundary condition (2.4) at  $x = 0$ . First, we assume that if the cytoneme shrinks to zero, then a new growing cytoneme is formed following an exponentially distributed waiting time due to nucleation. Note that we could also include a sticky boundary at  $x = L$ , in order to account for the possibility that when the cytoneme hits the boundary, its growth velocity  $v_+$  drops to zero and it sticks to the wall until transitioning to a shrinkage state at some rate  $r_L$ . Another generalization would be to take the search domain to extend beyond the array of cells ( $L > lK$ ). The probability  $P_k(t)$  that the cytoneme is captured by the  $k$ th target at time  $t$  satisfies the equation

$$\frac{dP_k}{dt} = \alpha_0 \int_{(k-1)l}^{kl} p(x, t) dx, \quad p = p_+ + p_- \quad (3.2)$$

Summing Eqs. (3.1a) and (3.1b) and then integrating with respect to  $x$  over the interval  $[0, L]$  shows that

$$\begin{aligned} \frac{d}{dt} \int_0^L p(x, t) dx &= - [v_+ p_+(x, t) - v_- p_-(x, t)]|_0^L \\ &\quad - \alpha_0 \int_0^L p(x, t) dx \end{aligned}$$

Given the boundary conditions (2.3) and (2.4), it follows that

$$\frac{d}{dt} \int_0^L p(x, t) dx + \sum_{k=0}^N \frac{dP_k}{dt} = 0,$$

which ensures conservation of total probability over all

events, that is

$$\int_0^L p(x, t) dx + \sum_{k=0}^N P_k(t) = 1. \quad (3.3)$$

We would like to determine the splitting probability  $\rho_k$  that the cytoneme is eventually captured by the  $k$ th target, where

$$\rho_k = \lim_{t \rightarrow \infty} P_k(t), \quad \sum_{k=1}^K \rho_k = 1. \quad (3.4)$$

Another quantity of interest is the conditional mean first passage time  $\tau_k$  for capture by the  $k$ th target.

### A. Conditional MFPT to reach $x = 0$ .

We first consider the conditional MFPT for a cytoneme to shrink back to the boundary at  $x = 0$ , having started in state  $(y, m)$  at time  $t = 0$  with  $m \in \{+, -\}$ . For the moment, assume that there is no nucleation effect and impose an absorbing boundary condition at  $x = 0$ , that is,  $p_-(0, t) = 0$ . We will use the backward version of Eqs. (3.1a) and (3.1b), which are given by

$$\frac{\partial q_+}{\partial t} = v_+ \frac{\partial q_+}{\partial y} - \alpha_- [q_+ - q_-] - \alpha_0 q_+, \quad (3.5a)$$

$$\frac{\partial q_-}{\partial t} = -v_- \frac{\partial q_-}{\partial y} + \alpha_+ [q_+ - q_-] - \alpha_0 q_-, \quad (3.5b)$$

where  $q_m(y, t) = p(x, n, t | y, m, 0)$  for a given final condition. We introduce the FPT

$$\begin{aligned} T_m^0(y) &= \inf\{t \geq 0; X(t) = 0, N(t) = -|X(0) = y, \\ &\quad N(0) = m\}. \end{aligned}$$

Note that  $T_m^0(y) = \infty$  means the cytoneme never shrinks back to the source cell before being captured by a target cell.

In order to calculate the conditional MFPT  $\tau_m^0 := \mathbb{E}[T_m^0(y) | T_m^0(y) < \infty]$ , we need to determine the corresponding splitting probability. Since the probability flux through the end  $x = 0$  is  $J_m^0(y, t) = v_- p(0, -, t | y, m, 0)$ , it follows that for  $0 < y < L$ , the probability  $\Pi_m^0(y, t)$  that the particle exits at  $x = 0$  after time  $t$ , having started in state  $(y, m)$ , is

$$\Pi_m^0(y, t) = \mathbb{P}[t < T_m^0(y) < \infty] = \int_t^\infty J_m^0(y, t') dt'. \quad (3.6)$$

Differentiating with respect to  $t$  gives

$$\frac{\partial \Pi_m^0(y, t)}{\partial t} = -J_m^0(y, t) = \int_t^\infty \frac{\partial J_m^0(y, t')}{\partial t'} dt'.$$

Hence, using the backward CK equation leads to the pair of equations

$$\frac{\partial \Pi_+^0}{\partial t} = v_+ \frac{\partial \Pi_+^0}{\partial y} - \alpha_- [\Pi_+^0 - \Pi_-^0] - \alpha_0 \Pi_+^0, \quad (3.7a)$$

$$\frac{\partial \Pi_-^0}{\partial t} = -v_- \frac{\partial \Pi_-^0}{\partial y} + \alpha_+ [\Pi_+^0 - \Pi_-^0] - \alpha_0 \Pi_-^0. \quad (3.7b)$$

In order to determine the boundary conditions at  $x = 0, L$ , note that if the cytoneme starts out in the shrinking phase at  $x = 0$ , it is immediately absorbed, whereas if it starts out at  $x = L$  in the growing phase it immediately transitions to the shrinkage phase. Hence,  $\Pi_-^0(0, t) = 1$  and  $\Pi_+^0(L, t) = \Pi_-^0(L, t)$ .

We can now define the hitting or splitting probability that the particle exits at  $x = 0$  rather than being captured by a target cell according to  $\pi_m^0(y) = \Pi_m^0(y, 0)$ . Since

$$\left. \frac{\partial \Pi_m^0(y, t)}{\partial t} \right|_{t=0} = -J_m^0(y, 0) = 0$$

for  $0 < y < L$ , we see that  $\pi_m^0$  satisfies the steady-state equations

$$0 = v_+ \frac{\partial \pi_+^0}{\partial y} - \alpha_- [\pi_+^0 - \pi_-^0] - \alpha_0 \pi_+^0, \quad (3.8a)$$

$$0 = -v_- \frac{\partial \pi_-^0}{\partial y} + \alpha_+ [\pi_+^0 - \pi_-^0] - \alpha_0 \pi_-^0, \quad (3.8b)$$

with boundary conditions  $\pi_-^0(0) = 1$  and  $\pi_+^0(L) = \pi_-^0(L)$ . It also follows that the probability that the cytoneme tip hits  $x = 0$  after time  $t$ , conditioned on not being captured by a target cell, is  $\mathbb{P}[t < T_m^0(y) | T_m^0(y) < \infty] = \Pi_m^0(y, t) / \Pi_m^0(y, 0)$ . Hence, the conditional MFPT satisfies

$$\begin{aligned} \omega_m^0(y) &:= \mathbb{E}[T_m^0(y) | T_m^0(y) < \infty] \\ &= - \int_0^\infty t \frac{\partial \mathbb{P}[t < T_m^0(y) | T_m^0(y) < \infty]}{\partial t} dt \\ &= \int_0^\infty \frac{\Pi_m^0(y, t)}{\pi_m^0(y, 0)} dt, \end{aligned}$$

Integrating Eqs. (3.7a) and (3.7b) with respect to  $t$  then gives

$$-\pi_+^0 = v_+ \frac{\partial \pi_+^0 \omega_+^0}{\partial y} - \alpha_- [\pi_+^0 \omega_+^0 - \pi_-^0 \omega_-^0] - \alpha_0 \pi_+^0 \omega_+^0, \quad (3.9a)$$

$$-\pi_-^0 = -v_- \frac{\partial \pi_-^0 \omega_-^0}{\partial y} + \alpha_+ [\pi_+^0 \omega_+^0 - \pi_-^0 \omega_-^0] - \alpha_0 \pi_-^0 \omega_-^0, \quad (3.9b)$$

with boundary conditions  $\pi_-^0(0) \omega_-^0(0) = 0$  and  $\pi_+^0(L) \omega_+^0(L) = \pi_-^0(L) \omega_-^0(L)$ .

## B. Conditional MFPT to be captured by a target before reaching $x = 0$ .

Next we consider the MFPT for the cytoneme tip to be captured by the  $k$ th target cell while in the growing phase, having started in state  $(y, m)$  at time  $t = 0$  and  $m \in \{+, -\}$ . It is convenient to introduce a new stochastic variable  $K(t) \in \{0, 1, \dots, K\}$  with  $K(t) = k$ ,  $1 \leq k \leq K$  indicating that the cytoneme is attached to the  $k$ th target cell at time  $t$  and  $K(t) = 0$  indicating that the cytoneme is not attached to any target cell. Following a similar sequence of steps as the previous case, we first introduce the FPT

$$\begin{aligned} T_m^k(y) &= \inf\{t \geq 0; (k-1)l < X(t) \leq kl, \\ &K(t) = k | X(0) = y, N(0) = m\}. \end{aligned}$$

The probability flux into the  $k$ th target cell is

$$J_m^k(y, t) = \alpha_0 \int_{(k-1)l}^{kl} p(x, n, t | y, m, 0) dx,$$

so that

$$\Pi_m^k(y, t) := \mathbb{P}[t < T_m^k(y) < \infty] = \int_t^\infty J_m^k(y, t') dt',$$

where  $\Pi_m^k(y, t)$  is the probability that the cytoneme tip is captured by the  $k$ th target cell after time  $t$ , having started in state  $(y, m)$ . Integrating Eqs. (3.5a) and (3.5b) over the interval  $(k-1)l < x \leq kl$  yields equation with the same structure as (3.7a) and (3.7b):

$$\frac{\partial \Pi_+^k}{\partial t} = v_+ \frac{\partial \Pi_+^k}{\partial y} - \alpha_- [\Pi_+^k - \Pi_-^k] - \alpha_0 \Pi_+^k, \quad (3.10a)$$

$$\frac{\partial \Pi_-^k}{\partial t} = -v_- \frac{\partial \Pi_-^k}{\partial y} + \alpha_+ [\Pi_+^k - \Pi_-^k] - \alpha_0 \Pi_-^k. \quad (3.10b)$$

The boundary conditions at  $x = 0, L$  can be determined using similar arguments to the previous example. The main difference is that if the cytoneme starts out in the shrinkage phase at  $x = 0$ , then it is never captured by a target cell. Hence,  $\Pi_-^k(0, t) = 0$  and  $\Pi_+^k(L, t) = \Pi_-^k(L, t)$ .

The splitting probability that the cytoneme tip is captured by the  $k$ th target cell rather than exiting through  $x = 0$  or being captured by another target cell is given by  $\pi_m^k(y) = \Pi_m^k(y, 0)$ . Since

$$\left. \frac{\partial \Pi_m^k(y, t)}{\partial t} \right|_{t=0} = -J_m^k(y, 0) = -\alpha_0 \chi_k(y),$$

where  $\chi_k(y)$  is the indicator function  $\chi_k(y) = 1$  if  $(k-1)l < y \leq kl$  and zero otherwise, it follows that

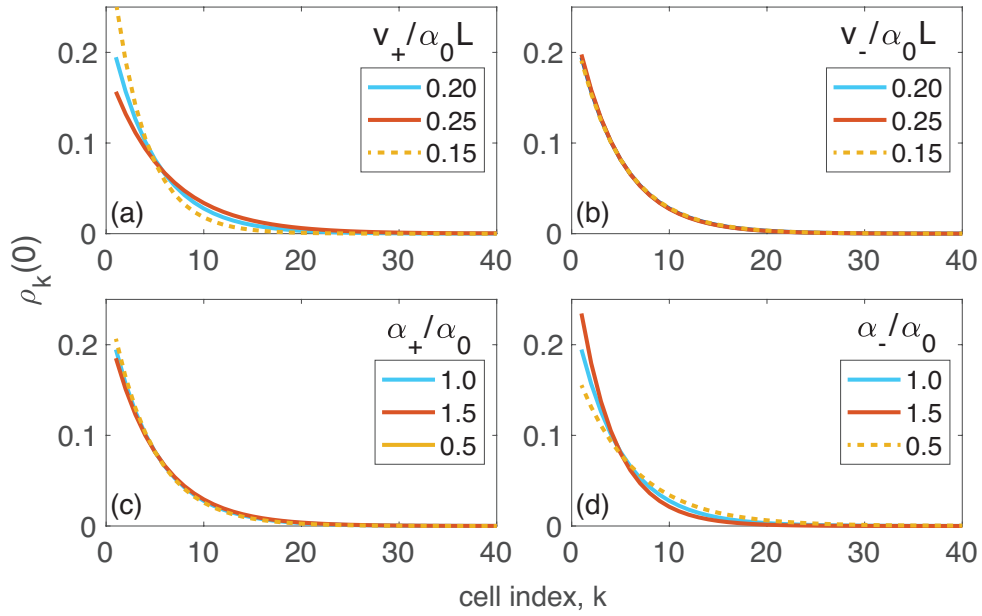


FIG. 4. Splitting probabilities of the search-and-capture model for a single cytoneme. (a,b) Plots of  $\rho_k(0)$  against  $k$ , see Eq.(3.14), for various dimensionless growth and shrinkage rates  $v_{\pm}/\alpha_0 L$ . (c,d) Corresponding plots for the relative transition rates  $\alpha_{\pm}/\alpha_0$ . Parameter values are as follows:  $v_{\pm}/\alpha_0 L = 0.2$ ,  $\alpha_{\pm}/\alpha_0 = 1$ , and  $K = 40$ .

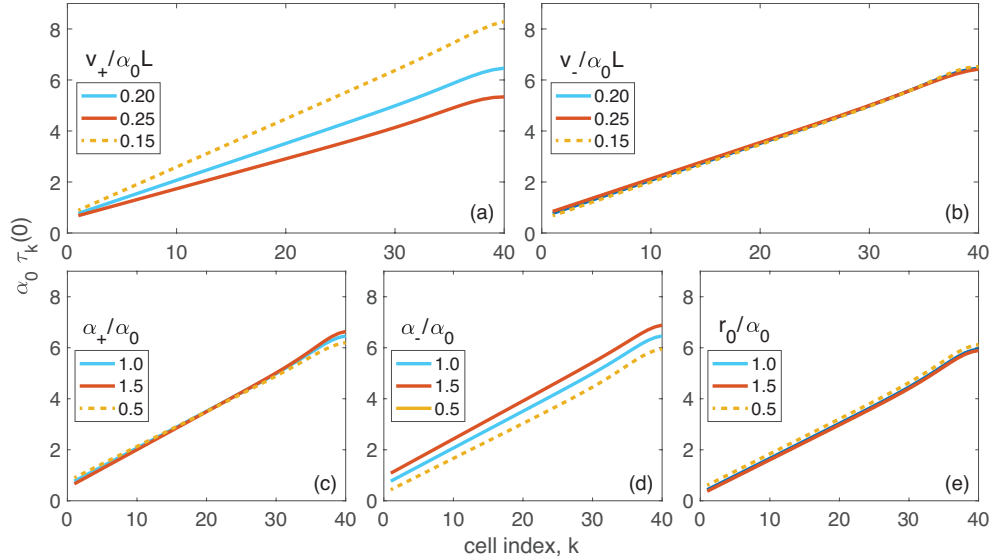


FIG. 5. Conditional MFPTs of the search-and-capture model for a single cytoneme and various parameters. (a,b) Plots of  $\alpha_0 \tau_k(0)$  against  $k$ , see Eq. (3.17), for various dimensionless growth and shrinkage rates  $v_{\pm}/\alpha_0 L$ . (c,d,e) Corresponding plots for the relative transition rates  $\alpha_{\pm}/\alpha_0$  and  $r_0/\alpha_0$ , respectively. Parameter values are the same as Fig. 4.

$\pi_m^k$  satisfies

$$-\alpha_0 \chi_k(y) = v_+ \frac{\partial \pi_+^k}{\partial y} - \alpha_- [\pi_+^k - \pi_-^k] - \alpha_0 \pi_+^k, \quad (3.11a)$$

$$-\alpha_0 \chi_k(y) = -v_- \frac{\partial \pi_-^k}{\partial y} + \alpha_+ [\pi_+^k - \pi_-^k] - \alpha_0 \pi_-^k, \quad (3.11b)$$

with boundary conditions  $\pi_-^k(0) = 0$  and  $\pi_+^k(L) = \pi_-^k(L)$ . The conditional probability that the cytoneme tip hits the  $k$ th target cell after time  $t$  is  $\mathbb{P}[t < T_m^k(y) | T_m^k(y) < \infty] = \Pi_m^k(y, t) / \Pi_m^k(y, 0)$ . Hence, the conditional MFPT satisfies

$$\omega_m^k(y) := \mathbb{E}[T_m^k(y) | T_m^k(y) < \infty] = \int_0^{\infty} \frac{\Pi_m^k(y, t)}{\Pi_m^k(y)} dt.$$

Integrating Eqs. (3.11a) and (3.11b) with respect to  $t$  yields equations identical in form to Eqs. (3.9a) and (3.9b):

$$-\pi_+^k = v_+ \frac{\partial \pi_+^k \omega_+^k}{\partial y} - \alpha_- [\pi_+^k \omega_+^k - \pi_-^k \omega_-^k] - \alpha_0 \pi_+^k \omega_+^k, \quad (3.12a)$$

$$-\pi_-^k = -v_- \frac{\partial \pi_-^k \omega_-^k}{\partial y} + \alpha_+ [\pi_+^k \omega_+^k - \pi_-^k \omega_-^k] - \alpha_0 \pi_-^k \omega_-^k, \quad (3.12b)$$

together with the boundary conditions  $\pi_-^k(0)\omega_-^k(0) = 0$  and  $\pi_+^k(L)\omega_+^k(L) = \pi_-^k(L)\omega_-^k(L)$ .

### C. Conditional MFPT to be captured by a target with nucleation at $x = 0$ .

Now suppose that we include a nucleating state at  $x = 0$  and impose the boundary conditions (2.3) and (2.4). We also assume that the cytoneme starts at  $y = 0$  in the growing phase  $m = 1$  and is eventually captured by the  $k$ th cytoneme with  $k$  fixed. Consider the following set of FPTs:

$$\mathcal{T}_k = \inf\{t > 0; (k-1)l < X(t) \leq kl, N(t) = 0\},$$

$$\mathcal{T}_0 = \inf\{t > 0; X(t) = 0, N(t) = -\},$$

$$\mathcal{R}_k = \inf\{t > 0; (k-1)l < X(\mathcal{T}_0 + t) \leq kl, N(\mathcal{T}_0 + t) = 0\},$$

for  $k = 1, 2, \dots, K$ , where we have suppressed the explicit dependence on the initial condition  $(y, +)$ . Next we introduce the sets

$$\Omega_k = \{\mathcal{T}_k < \infty\}, \quad \Gamma_k = \{\mathcal{T}_0 < \mathcal{T}_k < \infty\} \subset \Omega_k.$$

That is,  $\Omega_k$  is the set of all events for which the cytoneme is eventually captured by the  $k$ th target cell, and  $\Gamma_k$  is the subset of events in  $\Omega_k$  for which the cytoneme nucleates at least once. It immediately follows that

$$\Omega_k \setminus \Gamma_k = \{\mathcal{T}_k < \mathcal{T}_0 = \infty\}.$$

In other words,  $\Omega_k \setminus \Gamma_k$  is the set of all events for which the cytoneme is captured by the  $k$ th target cell without any nucleation.

In order to deal with the sticky boundary at  $x = 0$ , we will proceed along similar lines to section II. First, the splitting probability  $\rho_k(y)$  of capture by the  $k$ th cell, starting at position  $y$  in the growth phase, can be decomposed as

$$\rho_k(y) := \mathbb{P}[\Omega_k] = \mathbb{P}[\Omega_k \setminus \Gamma_k] + \mathbb{P}[\Gamma_k] = \pi_+^k(y) + \mathbb{P}[\Gamma_k]. \quad (3.13)$$

Moreover,

$$\mathbb{P}[\Gamma_k] = \mathbb{P}[\mathcal{T}_0 < \infty] \cdot \mathbb{P}[\mathcal{R}_k < \infty] = \pi_+^0(y) \mathbb{P}[\mathcal{R}_k < \infty].$$

We are assuming that the nucleation waiting time is finite. The strong Markov property means that  $\mathbb{P}[\mathcal{R}_k < \infty] = \rho_k(0)$ , so that Eq. (3.13) becomes

$$\rho_k(0) = \pi_+^k(0) + \pi_+^0(0) \rho_k(0).$$

Rearranging, we find that

$$\rho_k(0) = \frac{\pi_+^k(0)}{1 - \pi_+^0(0)}, \quad (3.14)$$

Second, we introduce the MFPT  $z_k(0) := \mathbb{E}[\mathcal{T}_k 1_{\Omega_k}]$ , which we decompose as

$$\begin{aligned} z_k(0) &= \mathbb{E}[\mathcal{T}_k 1_{\Omega_k \setminus \Gamma_k}] + \mathbb{E}[\mathcal{T}_k 1_{\Gamma_k}] \\ &= \pi_+^k(0) \omega_+^k(0) + \mathbb{E}[(\mathcal{T}_0 + \widehat{\mathcal{T}} + \mathcal{R}_k) 1_{\Gamma_k}], \\ &= \pi_+^k(0) \omega_+^k(0) + \pi_+^0(0) \rho_k(0) \left[ \omega_+^0(0) + \frac{1}{r_0} \right] \\ &\quad + \mathbb{E}[\mathcal{R}_k 1_{\Gamma_k}], \end{aligned} \quad (3.15)$$

where  $r_0$  is the rate of nucleation. From the strong Markov property, the conditional MFPT for  $\widehat{X}(t)$  to be captured by the  $k$ th target is  $z_k(0)/\rho_k(0)$ , so that

$$z_k(0) = \pi_+^k(0) \omega_+^k(0) + \pi_+^0(0) \rho_k(0) \left[ \omega_+^0(0) + \frac{1}{r_0} + \frac{z_k(0)}{\rho_k(0)} \right]. \quad (3.16)$$

Rearranging the above equation and using Eq. (3.14) yields

$$z_k(0) = \rho_k(0) \left[ \omega_+^k(0) + \frac{\pi_+^0(0)}{1 - \pi_+^0(0)} \left[ \omega_+^0(0) + \frac{1}{r_0} \right] \right]. \quad (3.17)$$

The corresponding conditional MFPT is then  $\tau_k(0) = z_k(0)/\rho_k(0)$ .

In Fig. 4 and Fig. 5 we show example plots of the splitting probability and conditional MFPT as a function of the target cell index  $k$ . One major observation is that both statistical quantities are quite robust with respect to changes in the dimensionless growth and shrinkage rates  $v_{\pm}/\alpha_0 L$ , and the relative transition rates  $\alpha_{\pm}/\alpha_0$ . There is, however, a greater sensitivity to variations in  $v_+/\alpha_0 L$  and  $\alpha_-/\alpha_0$ . Note that parameters are chosen to be consistent with experimentally measured values obtained in studies of cytoneme-mediated transport of Wnt morphogens zebrafish [8] and Shh in chicken [4]. Changes in the length of cytonemes are of the order  $0.1 \mu\text{m}/\text{s}$  and contacts are made every  $10^2 - 10^3$  seconds. Taking a typical cytoneme length of  $L \sim 100 \mu\text{m}$ , we obtain the following range for the dimensionless quantities  $v_{\pm}/\alpha_0 L \sim 0.1 - 1$ .

## IV. MULTIPLE SEARCH-AND-CAPTURE EVENTS

In section III we focused on the search-and-capture of a single cytoneme by a target cell, without specifying how morphogen is delivered to the cell once contact has been made. Motivated by the transport mechanism of Wnt in vertebrates [9], we will assume that a certain amount of morphogen (presumably loaded in vesicles) is located at the tip of the cytoneme, which is delivered to the target

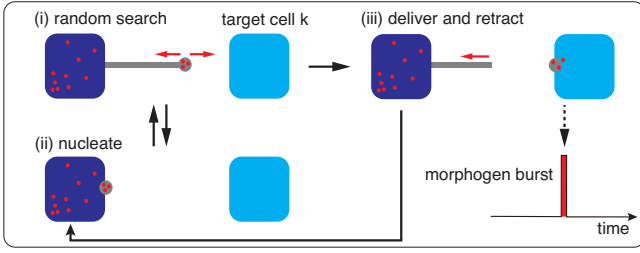


FIG. 6. Stages of a single search-and-capture process culminating in delivery of a burst of morphogen to the  $k$ th target cell. (i) Alternating periods of growth, shrinkage. (ii) Nucleation whenever the cytoneme shrinks to zero (iii) When a cytoneme is captured by a target cell, it delivers a morphogen burst and then retracts back to the nucleation site.

cell once contact is established. We will refer to this as a morphogen “burst.” After some fixed delay, the cytoneme then retracts back to the source cell, see Fig. 6. We wish to analyze how multiple rounds of search-and-capture, morphogen delivery, cytoneme retraction and nucleation events lead to the formation of a morphogen gradient. For simplicity, we will take the amount of morphogen transported by each nucleated cytoneme to be of fixed size  $d$ . (One could relax this assumption by modeling the loading of morphogens at the tip of a nucleated cytoneme as a stochastic process so that  $d$  is itself a random variable.)

Following section III, if a cytoneme starts at  $x = 0$  in the growth phase, then the probability that a single search-and-capture event delivers morphogen to the  $k$ th cell is  $\rho_k(0)$  and the conditional MFPT for the event is  $\tau_k(0) = z_k(0)/\rho_k(0)$ . The other  $K - 1$  target cells do not receive any morphogen. Now suppose that we have multiple search-and-capture events, under the simplifying assumptions that a captured cytoneme delivers its cargo without any delay, and then retracts back to  $x = 0$  at fixed time  $\tau_d$ , which is taken to be independent of the location of the target cell. (One could relax this assumption by taking  $\tau_d$  to be length dependent.) Let  $n = 1, \dots$  label the  $n$ th burst event and denote the target cell that receives the  $j$ th burst of morphogen by  $k_n$ . If  $T_n$  is the time of the  $n$ th burst, then

$$T_n = \tau_d + \mathcal{T}_{k_n} + T_{n-1}, \quad n \geq 1 \quad (4.1)$$

The corresponding inter-arrival times are

$$\Delta_n = \tau_d + \mathcal{T}_{k_n}, \quad n \geq 1.$$

In order to simplify the notation, we assume that the first round of search-and-capture starts with a cytoneme retracting back to  $x = 0$ . Finally, given an inter-arrival time  $\Delta$ , we denote the identity of the cell that captures the cytoneme by  $\mathcal{K}(\Delta)$ .

Consider a specific target cell  $k = \bar{k}$ . The cell will receive a sequence of morphogen bursts of size  $d_n$  at times  $T_n$  with  $d_n = 0$  if  $k_n \neq \bar{k}$  and  $d_n = d$  if  $k_n = \bar{k}$ . We

also include the effects of degradation, that is each morphogen delivered to the target cell degrades at a rate  $\kappa$ . We would like to determine the steady-state amount of morphogen in the long-time limit. We will proceed by reformulating the multiple search-and-capture model as a queuing process, see Fig. 7, analogous to the study of translational bursting in gene networks [25].

Queuing theory concerns the mathematical analysis of waiting lines formed by customers randomly arriving at some service station, and staying in the system until they receive service from a group of servers. Different types of queuing process are defined in terms of (i) the stochastic process underlying the arrival of customers, (ii) the distribution of the number of customers (batches) in each arrival, (iii) the stochastic process underlying the departure of customers (service-time distribution), and (iv) the number of servers. The above model of morphogen bursting can be mapped to a queuing process as follows: individual morphogens are analogous to customers, morphogen bursts correspond to customers arriving in batches  $X(t)$ , and the degradation of morphogens is the analog of customers exiting the system after being serviced. Thus, the waiting-time density for morphogen degradation is the analog of the service-time distribution. Finally, since the morphogens are degraded independently of each other, the effective number of servers in the corresponding queuing model is infinite, that is, the presence of other customers does not affect the service time of an individual customer.

The particular queuing model that maps to the model of morphogen bursting is the  $G/M/\infty$  system. Here the symbol  $G$  denotes a general inter-arrival time and target cell distribution  $F(t, k)$  for the cytoneme tip search-and-capture process. (In this section  $t$  denotes a waiting

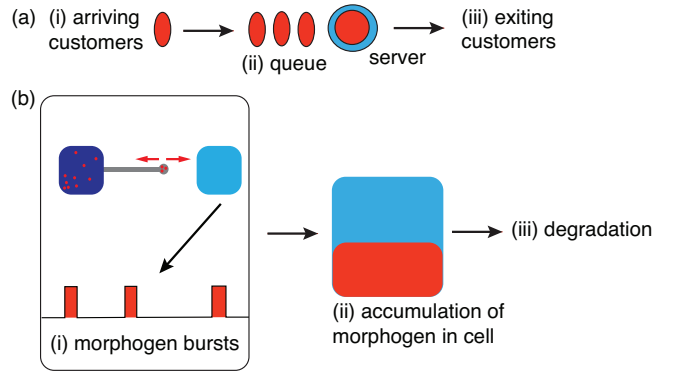


FIG. 7. Diagram illustrating the mapping between queuing theory and morphogen bursting. (a) Example of a single-server queue. (b) Morphogen bursting. Multiple search-and-capture events of a cytoneme generates a sequence of morphogen bursts within a target cell that is analogous to the arrival of customers in the queuing model. This results in the accumulation of morphogen within the cell, which is the analog of a queue. Degradation corresponds to exiting of customers after being serviced by an infinite number of servers.

time.) The symbol  $M$  stands for a Markovian or exponential service-time distribution  $H(t) = 1 - e^{-\kappa t}$  for morphogen degradation, and ‘ $\infty$ ’ denotes infinite servers. Before proceeding we need to specify how  $F(t, k)$  relates to the quantities calculated in section III. We can write

$$\begin{aligned} F(t, k) &= \mathbb{P}[\Delta < t, \mathcal{K}(\Delta) = k] \\ &= \mathbb{P}[\Delta < t, |\mathcal{K}(\Delta) = k| \mathbb{P}[\mathcal{K}(\Delta) = k] \\ &= \rho_k(0) \int_0^t f_k(\tau) d\tau \end{aligned} \quad (4.2)$$

where  $f_k(\tau)$  is the FPT density for the conditional MFPT of a single search-and-capture event that terminates at the  $k$ th cell. In particular,

$$\int_0^\infty \tau f_k(\tau) d\tau = \tau_k(0) + \tau_d. \quad (4.3)$$

### A. Moments of $G/M/\infty$ queuing model

Let  $N(t)$  be the number of busy servers at time  $t$ . This corresponds to the number of morphogens in the labeled cell  $\bar{k}$  that have not yet degraded. In terms of the sequence of arrival times  $T_n$  and cell identities  $k_n$ , we can write

$$N(t) = \sum_{n, 0 \leq T_n \leq t} \chi(t - T_n) \delta_{k_n \bar{k}}, \quad (4.4)$$

where

$$\chi(t - T_n) = \sum_{i=1}^d I(t - T_n, S_{ni}), \quad (4.5)$$

for

$$I(t - T_n, S_{ni}) = \begin{cases} 1 & \text{if } t - T_n \leq S_{ni} \\ 0 & \text{if } t - T_n > S_{ni} \end{cases}. \quad (4.6)$$

Here  $S_{ni}$ ,  $i = 1, \dots$ , is the service time of the  $i$ th member of a burst delivered to the cell  $\bar{k}$ .

Introduce the generating function

$$G(z, t) = \sum_{l=0}^{\infty} z^l \mathbb{P}[N(t) = l], \quad (4.7)$$

and the binomial moments

$$B_r(t) = \sum_{l=r}^{\infty} \frac{l!}{(l-r)!r!} \mathbb{P}[N(t) = l], \quad r = 1, 2, \dots \quad (4.8)$$

Suppose that the system is empty at time  $t = 0$ . We now derive an integral equation for the generating function  $G(z, t)$ . Conditioning the first arrival time by setting  $T_1 = y$ , we have

$$N(t) = \begin{cases} \chi(t - y) \delta_{k_1, \bar{k}} + N^*(t - y) & \text{if } y \leq t \\ 0 & \text{if } y > t \end{cases},$$

where  $N^*(t)$  has the same distribution as  $N(t)$ . Note that  $\chi(t - y) \delta_{k_1, \bar{k}}$  and  $N^*(t - y)$  are independent. Moreover,

$$\mathbb{P}[I(t - y, S_{1i}) = j] = [1 - H(t - y)] \delta_{j,1} + H(t - y) \delta_{j,0},$$

so it follows that

$$\sum_{j=0,1} z^j \mathbb{P}[I(t - y, S_{1i}) = j] = z + (1 - z)H(t - y).$$

Since  $I(t - y, S_{1i})$  for  $i = 1, 2, \dots, d$  are independent and identically distributed, the total expectation theorem yields

$$\begin{aligned} \mathbb{E}[z^{\chi(t - T_1) \delta_{k_1, \bar{k}}}] &= \mathbb{E} \left[ \mathbb{E}[z^{\chi(t - T_1) \delta_{k_1, \bar{k}}} | T_1 = y] \right] \\ &= \mathbb{E} \left[ \prod_{i=1}^b \mathbb{E}[z^{\delta_{k_1, \bar{k}} I(t - y, S_{1i})}] \right] \\ &= \int_0^\infty [z + (1 - z)H(t - y)]^d dF(y, \bar{k}). \end{aligned}$$

Another application of the total expectation theorem gives

$$\begin{aligned} G(z, t) &= \mathbb{E}[z^{N(t)}] = \mathbb{E} \left[ \mathbb{E}[z^{N(t)} | T_1 = y] \right] \\ &= \sum_{k=1}^K \int_t^\infty dF(y, k) \\ &\quad + \int_0^t [z + (1 - z)H(t - y)]^d G(z, t - y) dF(y, \bar{k}) \\ &\quad + \sum_{k \neq \bar{k}} \int_0^t G(z, t - y) dF(y, k). \end{aligned} \quad (4.9)$$

One can now obtain an iterative equation for the Binomial moments by differentiating Eq. (4.9) with respect to  $z$  and using

$$B_r(t) = \frac{1}{r!} \left. \frac{d^r G(z, t)}{dz^r} \right|_{z=1}$$

Since

$$\begin{aligned} \left. \frac{d^r}{dz^r} [z + (1 - z)H(t - y)]^d \right|_{z=1} \\ = \begin{cases} \frac{d!}{(d-r)!} [1 - H(t - y)]^r & \text{if } d \geq r \\ 0 & \text{if } d < r \end{cases}, \end{aligned}$$

we obtain the integral equation

$$\begin{aligned} B_r(t) &= \sum_{k=1}^K \int_0^t B_r(t - y) dF(y, k) + \sum_{l=1}^r \binom{d}{l} \\ &\quad \times \int_0^t B_{r-l}(t - y) [1 - H(t - y)]^l A_l dF(y, \bar{k}), \end{aligned}$$

where  $A_l = 1$  for  $l \leq d$  and  $A_l = 0$  for  $l > d$ . This can be written in the more compact form

$$B_r(t) = \sum_{k=1}^K \int_0^t B_r(t - y) dF(y, k) + \int_0^t \mathcal{H}_r(t - y) dF(y, \bar{k}), \quad (4.10)$$

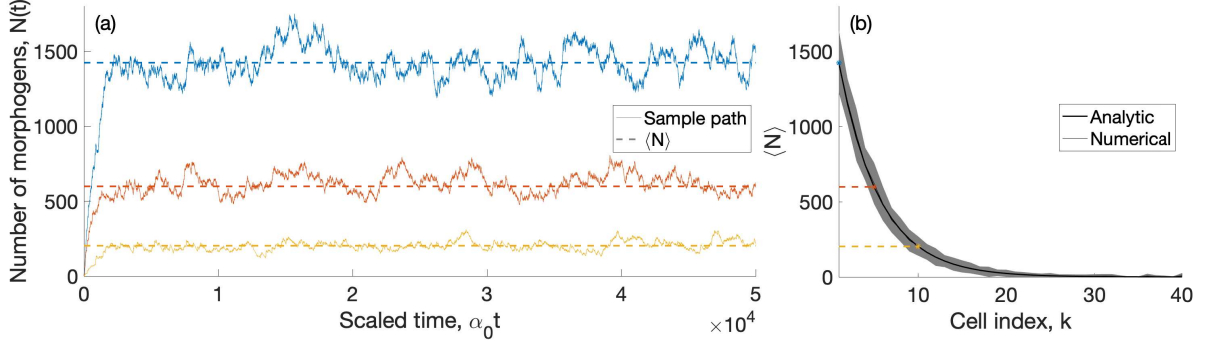


FIG. 8. Distribution of morphogens for multiple search-and-capture events and various target cells. (a) Sample paths (solid lines) and the steady-state mean (dashed lines) of  $N(t)$  for  $k = 1$  (blue/top lines),  $k = 5$  (orange/middle lines), and  $k = 10$  (yellow/bottom lines). (b) Plot of  $\langle N \rangle$  as a function of  $k$  obtained from Eq. (4.14) (solid curve), which is indistinguishable from the corresponding curve obtained using Monte-Carlo simulations. The gray shaded region indicates the standard deviation of  $N(t)$  as a function of  $k$ . Parameter values of a single search-and-capture event are the same as Fig. 4. Additional parameters of the multiple search-and-capture model are as follows:  $d = 10$ ,  $\kappa/\alpha_0 = 0.001$ ,  $r_0/\alpha_0 = 1$ , and  $\tau_d = 0$ .

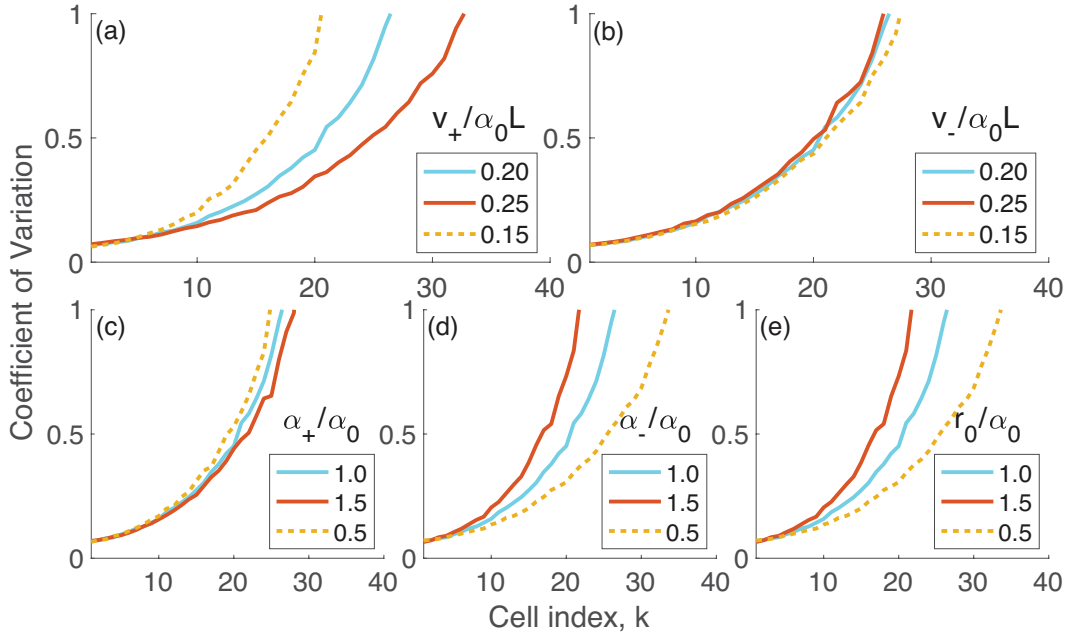


FIG. 9. Coefficient of variation (CV) of the steady-state distribution of  $N(t)$ . (a,b) Plots of CV against  $k$  for various dimensionless growth and shrinkage rates  $v_{\pm}/\alpha_0 L$ . (c,d,e) Corresponding plots for the relative transition rates  $\alpha_{\pm}/\alpha_0$  and  $r_0/\alpha_0$ . The CVs are calculated by performing Monte-Carlo simulations over 50 trials. Parameters are the same as Fig. 8.

where

$$\mathcal{H}_r(t) = \sum_{l=1}^r \binom{d}{l} A_l B_{r-l}(t) e^{-l\kappa t}.$$

In order to obtain the steady-state binomial moments, we Laplace transform Eq. (4.10) after making the substitution  $dF(y, k) = \rho_k(0) f_k(y) dy$ :

$$\widehat{B}_r(s) = \widehat{B}_r(s) \sum_{k=1}^K \rho_k(0) \widehat{f}_k(s) + \widehat{\mathcal{H}}_r(s) \rho_{\bar{k}}(0) \widehat{f}_{\bar{k}}(s),$$

which can be rearranged to give

$$\begin{aligned} \widehat{B}_r(s) &= \frac{\widehat{\mathcal{H}}_r(s) \rho_{\bar{k}}(0) \widehat{f}_{\bar{k}}(s)}{1 - \sum_{k=1}^K \rho_k(0) \widehat{f}_k(s)} \\ &= \frac{\rho_{\bar{k}}(0) \widehat{f}_{\bar{k}}(s)}{1 - \sum_{k=1}^K \rho_k(0) \widehat{f}_k(s)} \\ &\quad \times \sum_{l=1}^r \binom{d}{l} A_l \widehat{B}_{r-l}(s + l\kappa). \end{aligned} \quad (4.11)$$

Multiplying both sides by  $s$  and taking the limit  $s \rightarrow 0^+$  yields

$$\begin{aligned} B_r^* &:= \lim_{t \rightarrow \infty} B_r(t) = \lim_{s \rightarrow 0^+} s \widehat{B}_r(s) \\ &= \lim_{s \rightarrow 0^+} \frac{s \rho_{\bar{k}}(0) \widehat{f}_{\bar{k}}(s)}{1 - \sum_{k=1}^K \rho_k(0) \widehat{f}_k(s)} \sum_{l=1}^r \binom{d}{l} A_l \widehat{B}_{r-l}(l\kappa). \end{aligned}$$

Using the l'Hospital rule with respect to  $s$  and assuming the moments of  $F(t, k)$  are finite yields

$$\lambda_{\bar{k}} := \lim_{s \rightarrow 0^+} \frac{s \rho_{\bar{k}}(0) \widehat{f}_{\bar{k}}(s)}{1 - \sum_{k=1}^K \rho_k(0) \widehat{f}_k(s)} = \frac{\rho_{\bar{k}}(0)}{\sum_{k=1}^K z_k(0)}. \quad (4.12)$$

Hence, our final result is

$$B_r^* = \lambda_{\bar{k}} \sum_{l=1}^r \binom{d}{l} A_l \widehat{B}_{r-l}(l\kappa). \quad (4.13)$$

Eqs. (4.11) and (4.13) completely determine the steady-state binomial moments. In particular, since  $B_0(t) = 1$  and  $\widehat{B}_0(s) = 1/s$ , the mean number of morphogens in the target cell  $\bar{k}$  is

$$B_1^* \equiv \langle N \rangle = \frac{\lambda_{\bar{k}} d}{\kappa}, \quad (4.14)$$

Hence, we can interpret  $\lambda_{\bar{k}}$  as the mean rate at which a morphogen burst is delivered to the given target cell. Similarly,

$$\begin{aligned} B_2^* &\equiv \frac{1}{2}(\langle N^2 \rangle - \langle N \rangle^2) = \frac{1}{\lambda} \left( \widehat{B}_1(\kappa) d + \frac{A_2 d(d-1)}{4\kappa} \right) \\ &= \frac{d^2 \lambda_{\bar{k}}}{4\kappa} \left( \frac{2\rho_{\bar{k}}(0) \widehat{f}_{\bar{k}}(\kappa)}{1 - \sum_{k=1}^K \rho_k(0) \widehat{f}_k(\kappa)} + A_2 \right) - \frac{d A_2 \lambda_{\bar{k}}}{4\kappa}. \end{aligned} \quad (4.15)$$

which implies that the variance of the number of morphogens is a quadratic function of  $d$ :

$$\begin{aligned} \langle N^2 \rangle - \langle N \rangle^2 &= 2B_2^* + B_1^* - (B_1^*)^2 \\ &= C_2 d^2 + C_1 d, \end{aligned} \quad (4.16)$$

where

$$C_1 = \frac{(2 - A_2) \lambda_{\bar{k}}}{2\kappa} \quad (4.17)$$

$$C_2 = \frac{\lambda_{\bar{k}}}{2\kappa} \left( \frac{2\rho_{\bar{k}}(0) \widehat{f}_{\bar{k}}(\kappa)}{1 - \sum_{k=1}^K \rho_k(0) \widehat{f}_k(\kappa)} + A_2 \right) - \frac{\lambda_{\bar{k}}^2}{\kappa^2 2}. \quad (4.18)$$

Note that the coefficients are independent of  $d$ . The corresponding coefficient of variation (CV) satisfies

$$\text{CV}^2 = \widetilde{C}_2 + \frac{\widetilde{C}_1}{d}, \quad (4.19)$$

where  $\widetilde{C}_i = \kappa^2 C_i / \lambda_{\bar{k}}^2$  for  $i = 1, 2$ , and is an increasing function of  $\kappa$ .

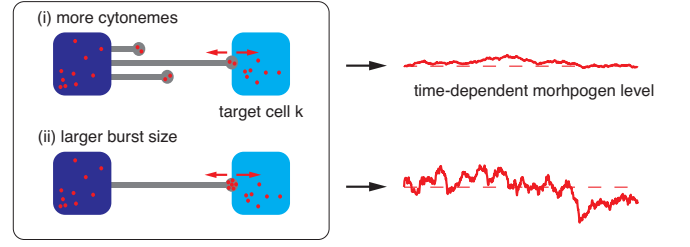


FIG. 10. Diagram illustrating the steady-state variance of the morphogen level. The variance is smaller for multiple cytonemes and a small burst size compared to a single cytoneme with a large burst size.

In Fig. 8 and Fig. 9 we present some example plots of the steady-state mean and variance of the number of morphogens in the array of target cells. Stochastic realizations of  $N(t)$  generate a noisy morphogen gradient. This noise is determined by the steady-state variance. In a similar fashion to the mean, the CV is more sensitive to changes in  $v_+/\alpha_0 L$  and  $\alpha_-/\alpha_0$ .

## B. Multiple independent cytonemes and optimal morphogen gradient amplification

Now suppose that the source cell has  $M$  independent nucleation sites so that multiple cytonemes deliver morphogens independently. Let  $N^m(t)$  be the number of morphogens present in the labeled target cell at time  $t$  that were delivered by the  $m$ th cytoneme and set

$$N^\Sigma(t) = \sum_{m=1}^M N^m(t).$$

Since  $N^m(t)$  are independent identically distributed random variables, we have the steady-state mean

$$\langle N^\Sigma \rangle = M \langle N \rangle = \frac{M d \lambda_{\bar{k}}}{\kappa}, \quad (4.20)$$

and variance

$$\sigma^2[N^\Sigma] = M \sigma^2[N] = M d (C_2 d + C_1). \quad (4.21)$$

Note that the steady-state mean  $\langle N^\Sigma \rangle$  depends on the product  $Md$ . Hence, for a given mean, one can reduce the variance by decreasing  $d$  and increasing  $M$  such that  $Md$  is fixed. That is, more frequent, smaller bursts generate a morphogen gradient with a smaller variance. This is illustrated in Fig. 10.

## V. SEARCH-AND-CAPTURE MODEL OF CHROMOSOME/MICROTUBULE ATTACHMENT

Having developed an alternative, probabilistic method for analyzing first passage time problems with sticky

boundaries in section II, which we applied to our model of cytoneme-based morphogenesis in section III, we now show how this method can also be used to simplify previous studies of search-and-capture models in cell mitosis. Although the latter are completely unrelated to models of cytoneme-based morphogenesis, they share some mathematical features which we highlight in this section. A crucial step in prometaphase, which is one of the major stages of cell mitosis, is the attachment of each chromosome to a microtubule of the mitotic spindle, which is the macromolecular structure responsible for segregating chromosomes to two daughter cells. According to the *search-and-capture* model of Kirschner and Mitchison [15], the underlying mechanism involves the nucleation of microtubules in random directions, which then grow and shrink dynamically in order to search space and eventually encounter a target kinetochore, see Fig. 11(a,b). The first theoretical study of the search-and-capture model was carried out by Holy and Leibler [35], which was then substantially extended in more recent work by Wollman et al [16]. The latter authors consider microtubules nucleating from two centrosomes, which could be located at the two focal points of an ellipsoid representing the cell shape, see Fig. 11(c). Pairs of chromosomes are linked together by kinetochores, which are the fixed targets of searching microtubules, and are distributed randomly around the equatorial plane. Each centrosome has hundreds of nucleating sites from which newly formed microtubules grow and shrink according to the Dogterom-Leibler model. It is assumed that microtubules from each nucleating site grow within a certain solid angle  $\Delta\Omega$ , which defines a search cone for the given nucleation site. It follows that any target falling within the search cone will subtend a solid angle at a point on the centrosome, where  $a$  is the cross-sectional area of the target and  $l$  is its distance from the centrosome. It follows that a microtubule originating from the nucleation site has a probability  $p_c = a/(l^2\Delta\Omega)$  of nucleating in the correct direction towards the target.

Wollman et al. [16] estimated the MFPT for a single target to be captured by microtubules nucleating from a single site under the simplifying assumption that the rescue rate following each catastrophe is zero ( $\alpha = 0$ ). This simplification avoided the need to deal with sticky boundaries.) A more detailed mathematical analysis of first passage time problems in the search-and-capture model has been developed by Gopalakrishnan and Govindan [19]. They allow for microtubule rescue, which means that one has to keep track of both nucleation events and collisions of a growing microtubule with the cell wall. This involves two separate sticky boundary conditions. The MFPT to capture a target was originally analyzed using forward methods [19], and subsequently solved more simply using backward methods [20]. Here we show how the analysis can be efficiently performed using the same probabilistic methods as used to study the cytoneme search-and-capture model.

Suppose that a microtubule is nucleated at a rate  $r_n$

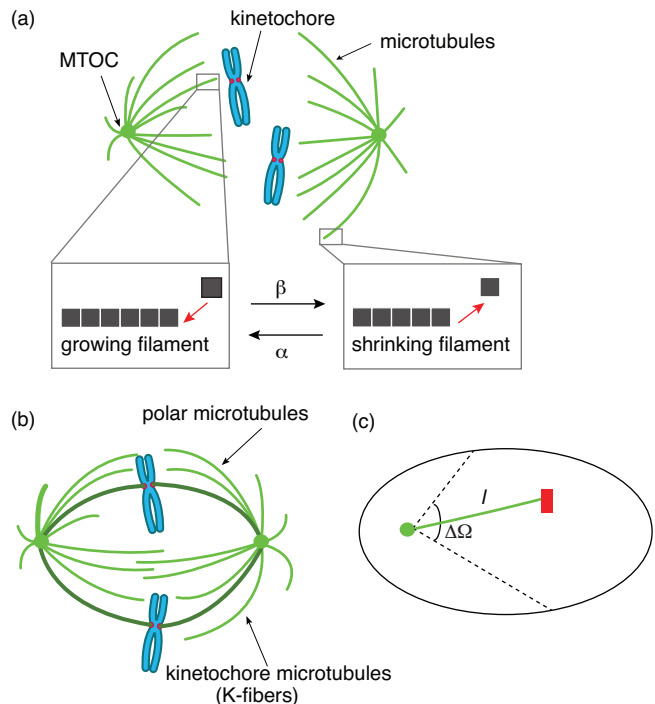


FIG. 11. Schematic diagram of the search-and-capture model based on microtubule dynamic instabilities. (a) During prometaphase microtubules randomly probe the cellular domain by alternating between growth and shrinkage phases until they capture the kinetochores. (b) At the end of prometaphase, all the kinetochores are attached to microtubules, one from each pole of the mitotic spindle, and are co-aligned along the mid-plane. (c) Illustration of the search cone of a nucleation site on one of the centrosomes of a cell, with the cell treated as an ellipsoid. A target falls within the search cone at a distance  $l$  from the site.

from a centrosome in an arbitrary direction that lies in a cone subtending a solid angle  $\Delta\Omega$ . As in the model of Wollman et al. [16], if the target is located at a distance  $d$  from the centrosome and has a cross-sectional area  $a$ , then it subtends a solid angle  $\Delta_c = a/d^2$  with respect to the centrosome. Hence, the probability of being nucleated in a direction that finds the target is  $p_c = \Delta\Omega_c/\Delta\Omega$ . We will assume that if the microtubule nucleates outside the target cone, which occurs with probability  $1 - p_c$ , then it can potentially grow until it hits a cell boundary at a distance  $L$  from the centrosome. (For simplicity, the search cone solid angle  $\Delta\Omega$  is taken to be sufficiently small so that the relevant region of the cell wall is approximately equidistant from the nucleation site.) Analogous to Fig. 1, whenever the microtubule hits the boundary at  $x = L$ , its growth velocity  $v_+$  drops to zero and it sticks to the wall until it transitions to a shrinkage state at a rate  $r_b$ .

Following [19], we decompose the total microtubule state space  $\Sigma$  as

$$\Sigma = N \cup A_b \cup B \cup A_c,$$

where  $N$  is the nucleation state,  $B$  is the state of being attached to the cell boundary,  $A_b$  are the active states that the microtubule is outside the target cone and has length  $X(t) \in (0, L)$ , and  $A_c$  are the active states that the microtubule is inside the target cone and has length  $X(t) \in (0, l)$ . Let  $S(t)$  denote the state of the microtubule at time  $t$ . If  $S(t) \in A_b$  then  $X(t)$  evolves according to the Dogtorem-Leibler model with sticky boundary conditions at  $x = 0, L$ . On the other hand, if  $S(t) \in A_c$  then  $X(t)$  evolves according to the Dogtorem-Leibler model with a sticky boundary condition at  $x = 0$  and an absorbing boundary condition at  $x = l$ . If  $S(t) = N$  then the microtubule transitions to a growing state, which either belongs to  $A_b$  with probability  $1 - p_c$  or belongs to  $A_c$  with probability  $p_c$ . The time  $\tilde{\tau}_n$  spent in state  $N$  is exponentially distributed with mean time  $r_n^{-1}$ . Similarly, the time  $\tilde{\tau}_b$  spent in state  $B$  is exponentially distributed with mean time  $r_b^{-1}$ . A schematic diagram of the search and capture model previously analyzed in Refs. [19, 20] is shown in Fig. 12.

Generalizing the analysis of Sect. 3.2, we define the following set of FPTs, assuming that the microtubule starts out in the nucleation state:

$$\begin{aligned} T &= \inf\{t \geq 0; X(t) = l\}, \\ T_b &= \inf\{t \geq 0; X(t + \tilde{\tau}_n) = l | S(\tilde{\tau}_n) \in A_b\}, \\ T_c &= \inf\{t \geq 0; X(t + \tilde{\tau}_n) = l | S(\tilde{\tau}_n) \in A_c\}, \\ S_b &= \inf\{t \geq 0; X(t + \tilde{\tau}_n) = 0 | S(\tilde{\tau}_n) \in A_b\}, \\ S_c &= \inf\{t \geq 0; X(t + \tilde{\tau}_n) = 0 | S(\tilde{\tau}_n) \in A_c\}, \\ \mathcal{T}_L &= \inf\{t \geq 0; X(t + \tilde{\tau}_n) = L | S(\tilde{\tau}_n) \in A_b\}, \\ \mathcal{R}_L &= \inf\{t \geq 0; X(t + \tilde{\tau}_b + \mathcal{T}_L) = 0\}. \end{aligned} \quad (5.22)$$

We also introduce the splitting probabilities and conditional MFPTs for the Dogtorem-Leibler model on the interval  $[0, L]$  with absorbing boundary conditions at both ends, see Sect.3. That is,  $\pi_m^L(y)$  and  $\bar{\pi}_m^L(y)$  are the splitting probabilities for being absorbed at the ends  $x = L$  and  $x = 0$  respectively, given the initial length  $y$  and initial growth/shrinkage state  $m = \pm$ . The corresponding conditional MFPTs are denoted by  $\omega_m^L(y)$  and  $\bar{\omega}_m^L(y)$ . (We make the length of the domain explicit.)

We immediately note that

$$\begin{aligned} \tau &:= \mathbb{E}[T] = (1 - p_c)\mathbb{E}[\tilde{\tau}_n + T_b] + p_c\mathbb{E}[\tilde{\tau}_n + T_c] \\ &= r_n^{-1} + (1 - p_c)\mathbb{E}[T_b] + p_c\mathbb{E}[T_c]. \end{aligned} \quad (5.23)$$

Introducing the set

$$\Omega_b = \{\mathcal{T}_L < S_b\},$$

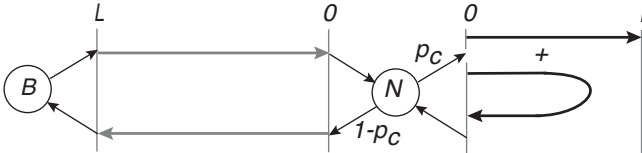


FIG. 12. Schematic illustration of the search-and-capture model analyzed in Ref. [19, 20].

we can perform the decomposition

$$\begin{aligned} \tau_b &:= \mathbb{E}[T_b] = \mathbb{E}[T_b 1_{\Omega_b^c}] + \mathbb{E}[T_b 1_{\Omega_b}] \\ &= \mathbb{E}[T_b 1_{\Omega_b^c}] + \mathbb{E}[(\mathcal{T}_L + \tilde{\tau}_b + \mathcal{R}_L + T) 1_{\Omega_b}]. \end{aligned}$$

Using the strong Markov property, we have

$$\begin{aligned} \tau_b &= \bar{\pi}_+^L(0) [\bar{\omega}_+^L(0) + \tau] + \pi_+^L(0) \left[ \omega_+^L(0) + \frac{1}{r_b} + \tau \right] \\ &\quad + \mathbb{E}[\mathcal{R}_L 1_{\Omega_b}] = \tau + \tau_L, \end{aligned} \quad (5.24)$$

with

$$\tau_L := \bar{\pi}_+^L(0) \bar{\omega}_+^L(0) + \pi_+^L(0) \left[ \omega_+^L(0) + \frac{1}{r_b} + \hat{\tau}_L \right], \quad (5.25)$$

and  $\hat{\tau}_L := \mathbb{E}[\mathcal{R}_L 1_{\Omega_b}]$ . In order to evaluate  $\hat{\tau}_L$ , note that the microtubule exits the state  $B$  in the shrinking phase and either reaches the state  $N$  without returning to  $B$ , which occurs with probability  $\bar{\pi}_-^L(L)$ , or returns to  $B$  first with probability  $\pi_-^L(L)$ . In the latter case it sticks to the boundary for a time  $\tilde{\tau}_b$  before exiting again. Thus,

$$\begin{aligned} \hat{\tau}_L &:= \mathbb{E}[\mathcal{R}_L 1_{\Omega_b}] \\ &= \bar{\pi}_-^L(L) \bar{\omega}_-^L(L) + \pi_-^L(L) (\omega_-^L(L) + r_b^{-1} + \hat{\tau}_L). \end{aligned} \quad (5.26)$$

The final step is to evaluate  $\mathbb{E}[T_c]$ . This is similar to the analysis of  $\tau_L$ . Exiting the state  $N$  in the growing phase and within the target search cone, the microtubule either reaches the target at  $x = l$  without first returning to  $N$ , which occurs with probability  $\pi_+^l(0)$ , or returns to  $N$  first with probability  $\bar{\pi}_+ = 1^l(0)$ . In the latter case the search process restarts. Thus,

$$\tau_c := \mathbb{E}[T_c] = \pi_+^l(0) \omega_+^l(0) + \bar{\pi}_+^l(0) [\bar{\omega}_+^l(0) + \tau] \quad (5.27)$$

Combining our various results gives the following implicit equation for the MFPT  $\tau$ :

$$\begin{aligned} \tau &= r_n^{-1} + p_c (\pi_+^l(0) \omega_+^l(0) + \bar{\pi}_+^l(0) [\bar{\omega}_+^l(0) + \tau]) \\ &\quad + (1 - p_c)(\tau_L + \tau), \end{aligned} \quad (5.28)$$

with  $\tau_L$  determined from Eqs. (5.25) and (5.26). Rearranging Eq.(5.28) yields the final explicit result

$$\begin{aligned} p_c \bar{\pi}_+^l(0) \tau &= r_n^{-1} + p_c (\pi_+^l(0) \omega_+^l(0) + \bar{\pi}_+^l(0) \bar{\omega}_+^l(0)) \\ &\quad + (1 - p_c) \tau_L. \end{aligned} \quad (5.29)$$

This recovers Eq. (67) of Ref. [20], and expresses the MFPT in terms of quantities that can be explicitly calculated. One advantage of our probabilistic approach is the small number of steps involved in deriving the formula for  $\tau$ . However, it does require identifying the appropriate set of stopping times as given by Eqs. (5.22).

## VI. DISCUSSION

In this paper, we developed a search-and-capture model of cytoneme-based morphogenesis, in which nucleating cytonemes from a source cell dynamically grow

and shrink along the surface of a one-dimensional array of target cells until making contact with one of the target cells. We calculated the splitting probabilities and the conditional MFPTs of a single cytoneme delivering a burst of morphogen to a target cell, and then used this to determine the steady-state mean and variance of the morphogen gradient in the case of multiple search-and-capture events. Using the result that the steady-state mean number of morphogens delivered to a target cell is given by Eq. (4.20), and assuming that the queuing process reaches steady-state faster than degradation, our model can be mapped onto the phenomenological dynamical model of Ref. [11]. That is, if  $u_k(t)$  is the mean morphogen level in the  $k$ th target cell at time  $t$ , then by taking

$$\frac{du_k(t)}{dt} = \frac{Md}{\sum_{l=1}^K z_l} \rho_k - \kappa u_k(t). \quad (6.1)$$

Here  $\kappa$  is the degradation rate of morphogen in a target cell and the first term on the right-hand side is the effective flux into the  $k$ th target cell. It follows that the effective accumulation time to the steady-state mean morphogen level is  $1/\kappa$ . Recall, however, that the CV is an increasing function of  $\kappa$ , suggesting that there may be some intermediate range of degradation rates that allow robust spatial pattern formation in a sufficiently short time.

Two more specific results emerged from our analysis. First, the search-and-capture model is robust with respect to changes in the dimensionless growth and shrinkage rates  $v_{\pm}/\alpha_0 L$  and the relative transition rates  $\alpha_{\pm}/\alpha_0$ . Second, given a fixed steady-state mean morphogen distribution, one can reduce the variance by increasing the number of cytonemes and reducing the load of each cytoneme. This predicts that for robust morphogen gradient formation, it is preferable for a source cell to extend a large number of cytonemes with small morphogen loads, rather than a few cytonemes with larger loads.

One simplifying assumption of our search-and-capture model is that the retraction time after delivery  $\tau_d$  is taken to be independent of the location of a target cell. If the retraction speed is constant, then we expect  $\tau_d$  to be inversely proportional to the distance between the nucleation site and the target cell. This space-dependent time delay could modify the steady-state mean and variance of the morphogen gradient. A second assumption is that the number of morphogen in each cytoneme tip is the same (fixed burst size). However, each time a cytoneme shrinks back to the source cell and subsequently renucleates, it is possible that morphogen is exchanged with the source cell so that the amount at the tip changes. This suggests treating the burst size as another random variable, which means that one has to solve a more general queuing model with correlated inter-arrival times and burst size distributions.

Given the complexity of the analysis, we focused on steady-state solutions of the queuing process in this paper. As in the case of diffusion-based models [36, 37], it is

also important to consider the dynamics of gradient formation, in order to address the question of whether or not the time to form the morphogen gradient is compatible with the time required for cell differentiation. For example, the latter process involves receptors measuring the local value of the morphogen concentration and translating this information into a corresponding change in the activation of its signaling pathways and gene expression. If gradient formation is relatively fast, then cell fate is determined by the steady-state value of the local morphogen concentration, otherwise the cell has to interpret a time-varying morphogen concentration. In our previous work on cytoneme-based morphogenesis in invertebrates [12, 13], which involves a different mechanism, we calculated the analog of the accumulation time considered in diffusion-based mechanisms, and showed that gradient formation was sufficiently fast. In future work we hope to develop a similar theory for the full search-and-capture model.

Finally note that, for simplicity, we developed our theory of cytoneme-based morphogenesis by considering a one-dimensional search-and-capture model. However, during embryogenesis, cytonemes typically grow and shrink in a higher-dimensional domain [9], rather than a one-dimensional array of cells. One such example is the Wg gradient in the *Drosophila* wing disc. Although we expect the search-and-capture model to form a stable morphogen gradient in higher dimensions, it is likely to take more time. This could be mitigated by the presence of a chemo-attractant gradient that guides the higher-dimensional search process. Indeed, the latter mechanism appears to play a role in the search-and-capture of kinetochores by microtubules during cell mitosis, which is a three-dimensional process. Using a combination of mathematical analysis and computer simulations, Wollman et al [16] have shown that unbiased search-and-capture for multiple chromosomes is not efficient enough to account for the duration of the prometaphase. On the other hand, if there exists a spatial gradient in some stabilizing factor that biases MT dynamics toward the chromosomes, then one obtains more realistic capture times [16]. One candidate molecule for acting as a stabilizing factor is Ran-GTP [38], which is also known to regulate actin polymerization [10]. In light of the possible role of Ran-GTP in cell mitosis, one prediction of our cytoneme-based model is that there exists an analogous cheom attractant present during embryogenesis.

## APPENDIX A: STOPPING TIMES AND THE STRONG MARKOV PROPERTY

In this appendix we present the basic definitions and results from probability theory used in the paper.

### A.1. Probability spaces and $\sigma$ -algebras

Consider a set of possible outcomes, which is denoted by the sample space  $\Omega$ . An event is defined to be a subset  $A$  of  $\Omega$ , which is some collection of single outcomes or elementary events  $\omega \in \Omega$ . In general not all subsets of  $\Omega$  can be treated as events so that the set of events forms a subcollection  $\mathcal{F}$  of all subsets. Within a probabilistic setting, this subcollection is required to be a so-called  *$\sigma$ -algebra*, with the following properties:

1.  $\emptyset \in \mathcal{F}$
2. if  $A_1, A_2, \dots \in \mathcal{F}$  then  $\cup_{i=1}^{\infty} A_i \in \mathcal{F}$
3. if  $A \in \mathcal{F}$  then  $\Omega \setminus A \in \mathcal{F}$

It can be shown that  $\sigma$ -algebras are closed under the operation of taking countable intersections. A *probability measure*  $\mathbb{P}$  on  $(\Omega, \mathcal{F})$  is a function  $\mathbb{P} : \mathcal{F} \rightarrow [0, 1]$  with

1.  $\mathbb{P}(\emptyset) = 0, \mathbb{P}(\Omega) = 1$
2. if  $A_i, A_j, \dots \in \mathcal{F}$  with  $A_i \cap A_j = \emptyset, i \neq j$ , then

$$\mathbb{P}(\cup_{i=1}^{\infty} A_i) = \sum_{i=1}^{\infty} \mathbb{P}(A_i).$$

The triple  $(\Omega, \mathcal{F}, \mathbb{P})$  is called a *probability space*.

Given a function  $f$  on the sample space  $\Omega$ , we can use the probability measure  $\mathbb{P}$  to define the integral of this function over a set  $A \in \mathcal{F}$  according to

$$f(A) = \int_A f(\omega) d\mathbb{P}(\omega).$$

If  $f(\omega) = 1$  for all  $\omega \in \Omega$ , then  $f(A) = \mathbb{P}(A)$ . Note that for certain choices of  $\sigma$ -algebra, it is necessary to consider measures other than the standard Lebesgue measure. However, we will not consider this technicality here. A *random variable* is a function  $X : \Omega \rightarrow \mathbb{R}$  such that

$$\{\omega \in \Omega : X(\omega) \leq x\} \in \mathcal{F}, \quad \forall x \in \mathbb{R}.$$

If this condition holds, then  $X$  is said to be  *$\mathcal{F}$ -measurable*. If  $X \in \mathbb{R}$  then we have a continuous random variable, whereas if  $X$  belongs to a countable set then it is said to be a discrete random variable. The *distribution function* of a random variable  $X$  is the function  $F : \mathbb{R} \rightarrow [0, 1]$  given by

$$F(x) = \text{Prob}(X \leq x) = \mathbb{P}(X^{-1}(-\infty, x]),$$

where  $X^{-1}(-\infty, x)$  is the set of events  $\omega$  for which  $X \leq x$ .

A stochastic process involves one or more random variables evolving in time. Each random variable will have an additional time label:  $X \rightarrow X_n, n \in \mathbb{Z}^+$  for discrete time processes and  $X \rightarrow X(t), t \in \mathbb{R}^+$  for continuous time processes. Roughly speaking, one can treat  $n$  (or  $t$ ) as a parameter so that for fixed  $n, X_n$  is a random variable in the above sense.

### A.2. Filtrations and stopping times

In the following we fix a probability space  $(\Omega, \mathcal{F}, \mathbb{P})$  and take  $T$  to be a subinterval of  $\mathbb{Z}^+$  (discrete time) or  $\mathbb{R}^+$  (continuous time). Suppose that there exists a collection  $(\mathcal{F}_t)_{t \in T}$  of  $\sigma$ -algebras  $\mathcal{F}_t \subseteq \mathcal{F}$ . The collection is said to be a filtration if  $\mathcal{F}_s \subseteq \mathcal{F}_t$  for all  $s \leq t$ . A stochastic process defined on  $(\Omega, \mathcal{F}, \mathbb{P})$  and indexed by  $T$  is called adapted to the filtration if for every  $t \in T$ , the random variable  $X_t$  is  $\mathcal{F}_t$ -measurable:

$$\{\omega \in \Omega : X_t(\omega) \leq x\} \in \mathcal{F}_t, \quad \forall x \in \mathbb{R}.$$

One can view a filtration as representing a flow of information, in the sense that the  $\sigma$ -algebra  $\mathcal{F}_t$  contains all possible events that can happen up to time  $t$ . The *canonical or natural filtration* generated by a stochastic process  $(X_t)_{t \in T}$  is given by

$$\mathcal{F}_t = \sigma(X_s, s \leq t),$$

which is the minimal filtration to which  $X$  is adapted. (If the filtration is not specified explicitly, it will be assumed to be the canonical filtration.) Roughly speaking, as  $t$  increases, the statistical information about a larger class of random variables is included within the  $\sigma$ -algebra  $\mathcal{F}_t$ , as one might expect from the evolution of a stochastic process.

A random variable  $\tau \in \mathbb{R}^+$  is called a *stopping time* with respect to the filtration  $(\mathcal{F}_t)_{t \in T}$  if for every  $t \in T$ , the event  $\{\tau \leq T\}$  is  $\mathcal{F}_t$ -measurable. If  $\tau < \infty$  almost surely, then  $\tau$  is called a finite stopping time. Heuristically speaking,  $\tau$  is a stopping time if for every  $t \in T$  we can completely determine whether or not  $\tau$  has occurred before time  $t$  using the information known up to time  $t$ . A common example is the *first passage time* for a stochastic process  $(X_t)$  in  $\mathbb{R}^d$  adapted to a filtration  $(\mathcal{F}_t)$ . Let  $A$  be closed subset of  $\mathbb{R}^d$  and define

$$\tau_A = \inf\{t \geq 0 : X_t \in A\}$$

In order to establish that  $\tau_A$  is a stopping time, introduce the sequence  $\{t_i\}_{i=1}^{\infty}$  dense on  $\mathbb{R}^+$ , and the sets

$$A_n = \left\{x \mid d(x, A) < \frac{1}{n}\right\},$$

where  $d(x, A)$  is a distance function (minimum Euclidean distance of  $x$  from the set  $A$ ). The event

$$\{\tau_A \leq t\} = \cap_{n=1}^{\infty} \cup_{t_i \leq t} \{X_{t_i} \in A_n\}$$

belongs to  $\mathcal{F}_t$  since each event  $\{X_{t_i} \in A_n\} \in \mathcal{F}_{t_i}$ .

### A.3. Strong Markov property

A stochastic process  $(X_t)$  adapted to a filtration  $(\mathcal{F}_t)$  is said to have the *Markov property* if the conditional probability distribution of future states of the process

(conditional on both past and present states) depends only upon the present state, not on the sequence of events that preceded it. That is, for all  $t' > t$  we have

$$\mathbb{P}[X_{t'} \leq x | X_s, s \leq t] = \mathbb{P}[X_{t'} \leq x | X_t].$$

The *strong Markov property* is similar to the Markov property, except that the “present” is defined in terms of a stopping time. That is, given any finite-valued stopping time  $\tau$  with respect to the natural filtration of  $X$ , if the stochastic process  $Y(t) = X(t+\tau) - X(\tau)$  is independent of  $\{X(s), s < \tau\}$  and has the same distribution as  $\hat{Y}(t) = X(t) - X(0)$  then  $X$  is said to satisfy the strong Markov property.

## APPENDIX B: EXPLICIT SOLUTIONS OF THE CONDITIONAL MFPTS

We first find a concise expression for the conditional MFPTs to reach  $x = 0$ . Non-dimensionalizing (3.7a) and (3.7b)

$$0 = \mathbf{v}_+ \frac{\partial \pi_+^0}{\partial y} - \mathbf{a}_- [\pi_+^0 - \pi_-^0] - \pi_+^0, \quad (\text{B.1a})$$

$$0 = -\mathbf{v}_- \frac{\partial \pi_-^0}{\partial y} + \mathbf{a}_+ [\pi_+^0 - \pi_-^0] - \pi_-^0, \quad (\text{B.1b})$$

for  $0 < y < 1$  where

$$\mathbf{v}_\pm = \frac{v_\pm}{\alpha_0 L}, \quad \mathbf{a}_\pm = \frac{\alpha_\pm}{\alpha_0},$$

and defining the following operator

$$\mathbb{L} = \left[ \begin{array}{cc} \mathbf{v}_+ \partial_y - \mathbf{a}_- - 1 & \mathbf{a}_- \\ \mathbf{a}_+ & -\mathbf{v}_- \partial_y - \mathbf{a}_+ - 1 \end{array} \right].$$

$$\begin{aligned} \eta_+^0(0) &= \eta_+^{0,h}(0) = \frac{\theta_2 - \theta_1}{\mathcal{N}} \left[ \eta_+^{0,p}(1) - \eta_-^{0,p}(1) \right] \\ &= \frac{1}{\mathcal{N}^2} \left( \frac{1}{\mathbf{v}_+} + \frac{1}{\mathbf{v}_-} \right) \left\{ \begin{array}{l} [(1 - \theta_1)^2 \theta_2 e^{\Lambda_1} + (1 - \theta_2)^2 \theta_1 e^{\Lambda_2}] \cdot \frac{e^{\Lambda_2} - e^{\Lambda_1}}{\Lambda_2 - \Lambda_1} \\ -(1 - \theta_1)(1 - \theta_2)(\theta_1 + \theta_2) e^{\Lambda_1 + \Lambda_2} \end{array} \right\}. \end{aligned} \quad (\text{B.5})$$

The corresponding conditional MFPT is therefore  $\omega_+^0(0) = \eta_+^0(0) / [\alpha_0 \pi_+^0(0)]$ .

In order to determine an exact solution of the conditional MFPT to be captured by the  $k$ th target cell before the nucleation, we again apply the variation of parameters. Its splitting probability satisfies

$$-\chi_k(y) = \mathbb{L}\pi^k(y), \quad 0 < y < 1, \quad (\text{B.6})$$

where  $\pi^k(y) = [\pi_+^k(y), \pi_-^k(y)]$  with boundary conditions  $\pi_-^k(0) = 0$  and  $\pi_+^k(1) = \pi_-^k(1)$ . Using the variation of parameters, one can find the particular solution of (B.6) and denote by  $\pi^{k,p}(y)$ . It satisfies  $\pi^{k,p}(0) = 0$ . In the same fashion for (B.5), we have

$$\pi_+^k(0) = \pi_+^{k,p} = \frac{\theta_2 - \theta_1}{\mathcal{N}} \left[ \pi_+^{k,p}(1) - \pi_-^{k,p}(1) \right] = \frac{1}{\mathcal{N}} \left[ \mathcal{E} \left( \frac{k-1}{K} \right) - \mathcal{E} \left( \frac{k}{K} \right) \right], \quad (\text{B.7})$$

where

$$\mathcal{E}(y) = \frac{1 - \theta_2}{\Lambda_2} \left( \frac{\theta_1}{\mathbf{v}_+} + \frac{1}{\mathbf{v}_-} \right) e^{\Lambda_2(1-y)} - \frac{1 - \theta_1}{\Lambda_1} \left( \frac{\theta_2}{\mathbf{v}_+} + \frac{1}{\mathbf{v}_-} \right) e^{\Lambda_1(1-y)}.$$

It follows that

$$0 = \mathbb{L}\pi^0(y), \quad (\text{B.2})$$

where  $\pi^0(y) = [\pi_+^0(y), \pi_-^0(y)]$  with boundary conditions  $\pi_-^0(0) = 1$  and  $\pi_-^0(1) = \pi_+^0(1)$ . By solving the systems of ODE (B.2) gives

$$\pi_+^0(0) = \frac{(1 - \theta_2)e^{\Lambda_2} - (1 - \theta_1)e^{\Lambda_1}}{\mathcal{N}}, \quad (\text{B.3})$$

where  $\Lambda_1 > \Lambda_2$  are the eigenvalues of operator  $\mathbb{L}$  satisfying

$$[\mathbf{v}_+ \Lambda - (1 + \mathbf{a}_-)][\mathbf{v}_- \Lambda + \mathbf{a}_+ + 1] + \mathbf{a}_+ \mathbf{a}_- = 0.$$

Here  $\theta_{1,2} = [-\mathbf{v}_+ \Lambda_{1,2} + \mathbf{a}_- + 1] / \mathbf{a}_-$  and  $\mathcal{N} = \theta_1(1 - \theta_2)e^{\Lambda_2} - \theta_2(1 - \theta_1)e^{\Lambda_1}$ .

One can write (3.9a) and (3.9b) using the operator

$$-\pi^0(y) = \mathbb{L}\eta^0(y), \quad (\text{B.4})$$

where  $\eta^0 = \alpha_0[\pi_+^0(y)\omega_+^0(y), \pi_-^0(y)\omega_-^0(y)]$  with boundary conditions  $\eta_-^0(0) = 0$  and  $\eta_-^0(1) = \eta_+^0(1)$ . Since (B.4) is an inhomogeneous version of Eq. (B.2), then one can find the particular solution  $\eta^{0,p}(y)$  by the variation of parameters with  $\eta^{0,p}(0) = 0$ . Then the corresponding homogeneous solution  $\eta^{0,h}(y) = \eta^0(y) - \eta^{0,p}(y)$  satisfies  $0 = \mathbb{L}\eta^{0,h}(y)$ , with boundary conditions  $\eta_-^{0,p}(0) = 0$  and  $\eta_+^{0,h}(1) + \eta_+^{0,p}(1) = \eta_-^{0,h}(1) + \eta_-^{0,p}(1)$ . It follows that

We determine the corresponding conditional MFPT by following the same method we used to get (B.5). Then one can have the explicit form of MFPT

$$\eta_+^k(0) = \frac{\pi_+^k(0)}{\mathcal{N}(\theta_2 - \theta_1)} \left\{ \begin{aligned} & \theta_1 \theta_2 (2 - \theta_1 - \theta_2) \left( \frac{1}{v_+} + \frac{1}{v_-} \right) \frac{e^{\Lambda_1 - \Lambda_2}}{\Lambda_1 - \Lambda_2} \\ & - \left[ (1 - \theta_1) \theta_2 \left( \frac{\theta_2}{v_+} + \frac{\theta_1}{v_-} \right) e^{\Lambda_1} + (1 - \theta_2) \theta_1 \left( \frac{\theta_1}{v_+} + \frac{\theta_2}{v_-} \right) e^{\Lambda_2} \right] \end{aligned} \right\} \\ + \frac{1}{\mathcal{N}(\theta_2 - \theta_1)} \left[ \widehat{\mathcal{E}} \left( \frac{k-1}{K} \right) - \widehat{\mathcal{E}} \left( \frac{k}{K} \right) \right], \quad (\text{B.8})$$

where  $\widehat{\mathcal{E}}(y) = \mathcal{F}_{12}(y) + \mathcal{F}_{21}(y)$  and

$$\mathcal{F}_{ij}(y) = (1 - \theta_i) \left\{ \begin{aligned} & \frac{1}{\Lambda_i} \left( \frac{\theta_j}{v_+} + \frac{\theta_i}{v_-} \right) \left( \frac{\theta_j}{v_+} + \frac{1}{v_-} \right) \left( 1 - \frac{1}{\Lambda_i} - y \right) e^{\Lambda_i(1-y)} \\ & - \frac{\theta_j}{\Lambda_j} \left( \frac{1}{v_+} + \frac{1}{v_-} \right) \left( \frac{\theta_j}{v_+} + \frac{1}{v_-} \right) \left[ \frac{e^{\Lambda_i(1-y)} - e^{\Lambda_j(1-y)}}{\Lambda_i - \Lambda_j} - \frac{e^{\Lambda_i(1-y)}}{\Lambda_i} \right] \end{aligned} \right\}.$$

Its corresponding conditional MFPT becomes  $\omega_+^k(0) = \eta_+^k(0) / [\alpha_0 \pi_+^k(0)]$ .

## ACKNOWLEDGEMENTS

PCB was supported by the National Science Foundation (DMS-1613048).

- 
- [1] S. Roy, F. Hsiung and T. B. Kornberg, Specificity of *Drosophila* cytonemes for distinct signaling pathways. *Science* **33** 354-358 (2011).
  - [2] A. C. Gradilla and I. Guerrero, Cytoneme-mediated cell-to-cell signaling during development. *Cell Tissue Res.* **352** 59-66 (2013).
  - [3] M. Bischoff, A. C. Gradilla, I. Seijo, G. Andres, C. Rodriguez-Navas, L. Gonzalez-Mendez and I. Guerrero, Cytonemes are required for the establishment of a normal Hedgehog morphogen gradient in *Drosophila* epithelia. *Nat Cell Biol* **15** 1269-1281 (2013).
  - [4] T. A. Sanders, E. Llagostera and M. Barna, Specialized filopodia direct long-range transport of SHH during vertebrate tissue patterning. *Nature* **497** 628-632 (2013).
  - [5] T. B. Kornberg, Cytonemes and the dispersion of morphogens. *WIREs Dev Biol* **3** 445-463 (2014).
  - [6] T. B. Kornberg and S. Roy, Cytonemes as specialized signaling filopodia. *Development* **141** 729-736 (2014).
  - [7] C. L. Fairchild and M. Barna, Specialized filopodia: at the tip of morphogen transport and vertebrate tissue patterning. *Curr. Opin. Genet. Dev.* **27** 67-73 (2014).
  - [8] E. Stanganello, A. I. H. Hagemann, B. Mattes, C. Sinner, D. Meyen, S. Weber, A. Schug, E. Raz and S. Scholpp, Filopodia-based Wnt transport during vertebrate tissue patterning. *Nat. Comm.* **6** 5846 (2015).
  - [9] E. Stanganello and S. Scholpp, Role of cytonemes in Wnt transport. *J. Cell Sci.* **129** 665-672 (2016).
  - [10] F. Prols, Sagar and M. Scaal, Signaling filopodia in vertebrate embryonic development. *Cell Mol Life Sci* **73** 961-974 (2016).
  - [11] H. Teimouri and A. B. Kolomeisky, New model for understanding mechanisms of biological signaling: direct transport via cytonemes. *J. Phys. Chem. Lett.* **7** 180-185 (2016).
  - [12] P. C. Bressloff and H. Kim, Bidirectional transport model of morphogen gradient formation via cytonemes. *Phys. Biol.* **15** 026010 (2018).
  - [13] H. Kim and P. C. Bressloff, Direct vs. synaptic contacts in a mathematical model of cytoneme-based morphogen gradient formation. *SIAM J. Appl. Math* **78** 2323-2347 (2018).
  - [14] T. L. Hill, Theoretical problems related to the attachment of microtubules to kinetochores. *Proc. Natl. Acad. Sci. U. S. A.* **82**, 4404-4408 (1985).
  - [15] M. Kirschner and T. Mitchison, Beyond self-assembly: from microtubules to morphogenesis. *Cell* **45**, 329-342 (1986).
  - [16] R. Wollman, E. N. Cytrynbaum, J. T. Jones, T. Meyer, J. M. Scholey and A. Mogilner, Efficient chromosome capture requires a bias in the 'search-and-capture' process during mitotic-spindle assembly. *Current Biology* **15**, 828-832 (2005).
  - [17] T. J. Mitchison and M. W. Kirschner, Dynamic instability of microtubule growth. *Nature* **312** 237-242 (1984).
  - [18] M. Dogterom and S. Leibler, Physical aspects of the growth and regulation of microtubule structures. *Phys. Rev. Lett.* **70** 1347-1350 (1993).
  - [19] M. Gopalakrishnan and B. S. Govindan, A first-passage-time theory for search and capture of chromosomes by microtubules in mitosis. *Bull. Math. Biol.* **73** 2483-2506 (2011).
  - [20] B. M. Mulder, Microtubules interacting with a boundary: Mean length and mean first-passage times. *Phys. Rev. E* **86** 011902 (2012).
  - [21] B. Zelinski, N. Muller and J. Kierfeld, Dynamics and length distribution of microtubules under force and confinement. *Phys. Rev. E* **86** 041918 (2012).
  - [22] M. Zeitz and J. Kierfeld, Feedback mechanism for microtubule length regulation by stathmin gradients. *Biophys.*

- J. **107** 2860-2871 (2014).
- [23] L. Angelani, Confined run-and-tumble swimmers in one dimension. *J. Phys. A* **50** 325601 (2017).
- [24] S. Redner, A guide to first-passage processes. Cambridge University Press, Cambridge, UK (2001).
- [25] N. Kumar, A. Singh A and R. V. Kulkarni, Transcriptional bursting in gene expression: analytical results for general stochastic models. *PLoS Comp. Biol.* **11** e1004292 (2015).
- [26] R. Durrett, Probability: Theory and examples. Cambridge series in statistical and probabilistic mathematics (2010).
- [27] P. C. Bressloff and S. D. Lawley, Escape from subcellular domains with randomly switching boundaries. *Multiscale Model. Simul.* **13** 1420-1455 (2015).
- [28] P. C. Bressloff and S. D. Lawley, Diffusion on a tree with stochastically-gated nodes. *J. Phys. A.* **49** 245601 (2016).
- [29] I. Bena, Dichotomous Markov noise: exact results for out-of-equilibrium systems. *Int. J. Mod. Phys. B* **20** 2825 (2006).
- [30] C. W. Gardiner, Handbook of stochastic methods, 4th edition. Springer, Berlin (2009).
- [31] P. C. Bressloff, Stochastic Processes in Cell Biology Springer Berlin (2014).
- [32] D. J. Bico, Green's functions and first passage time distributions for dynamic instability of microtubules. *Phys. Rev. E* **56** 6656-6667 (1997).
- [33] L. Angelani L, Run-and-tumble particles, telegrapher's equation and absorption problems with partially reflecting boundaries. *J. Phys. A* **48** 495003 (2015).
- [34] T. Hillen and A. Swan, The diffusion limit of transport equations in biology In: *Mathematical Models and Methods for Living Systems*, L. Preziosi et al (eds.) 3-129 (2016).
- [35] T. E. Holy and S. Leibler, Dynamic instability of microtubules as an efficient way to search in space. *Proc. Natl. Acad. Sci. U. S. A.* **91**, 5682-5685 (1994).
- [36] A. M. Berezhkovskii, C. Sample and S. Y. Shvartsman. How long does it take to establish a morphogen gradient? *Biophys J* **99** L59-L61 (2010).
- [37] A. M. Berezhkovskii, C. Sample and S. Y. Shvartsman. Formation of morphogen gradients: local accumulation time. *Phys Rev E* **83** 051906 (2011).
- [38] R. E. Carazo-Salas, et al. Ran-GTP coordinates regulation of microtubule nucleation and dynamics during mitotic-spindle assembly. *Nat. Cell Biol.* **3**, 228-234 (2001).